

Emergence of a linear tracer source from air concentration measurements

J.-P. Issartel

Emergence of a linear tracer source from air concentration measurements

J.-P. Issartel

Centre d'Enseignement et de Recherche en Environnement Atmosphérique, unité mixte Ecole Nationale des Ponts et Chaussées – Electricité de France, France Projet CLIME, équipe mixte Institut National de Recherche en Informatique et en Automatique – Ecole Nationale des Ponts et Chaussées, France

Received: 30 March 2004 – Accepted: 19 April 2004 – Published: 12 May 2004

Correspondence to: J.-P. Issartel (issartel@cerea.enpc.fr)

Title Page

Abstract

Introduction

Conclusions

References

Tables

Figures

⏪

⏩

◀

▶

Back

Close

Full Screen / Esc

Print Version

Interactive Discussion

Abstract

The measurement of atmospheric concentrations by a monitoring network is potentially a useful tool investigated for the identification of the widespread sources of trace species. The paper addresses inversion strategies using base functions multiplicatively deduced from the concentrations adjoint to the measurements. This follows the concept of illumination: the various regions are well, poorly or not seen at all. With ordinary adjoint functions the illumination becomes excessive close to the detectors. This may be corrected by attributing each point of the space time domain a geometric weight. After stating the statistical implications, the choice of this renormalising function is shown to be constrained by an unambiguous formal criterion. The expectable values of the measurements are distinguished from the measurement errors. The entropic nature of the criterion is explained; it amounts to evenly distribute the information between the points organised with their weights as a “known domain” describing the influence of the measurements. Finally the criterion is shown to coincide with the definition of the pure states of quantum statistics, and this interpretation is investigated to describe the influence of the measurement uncertainties on the quality of a source estimate. The theory is illustrated by calculations performed with the experimental source ETEX1.

1. Introduction

The atmospheric transport of tracers, especially the linear ones, is an active domain (Gallardo et al., 2002; Clerbaux et al., 2003; Baklanov and Mahura, 2004) with many investigations about the inverse problems (Bousquet et al., 2000; Rödenbeck et al., 2003). The natural interpretation of a measurement goes through its adjoint function (Marchuk, 1992; Robertson and Persson, 1993; Penenko and Baklanov, 2001). The localisation of accidental point sources has been widely studied (Sharan et al., 1995; Pudykiewicz, 1998; Seibert, 2001; Roussel et al., 2002; Issartel and Baverel, 2003; Penenko et al., 2002). The reconstruction of the widespread sources of such species

Emergence of a linear tracer source from air concentration measurements

J.-P. Issartel

Title Page

Abstract

Introduction

Conclusions

References

Tables

Figures

⏪

⏩

◀

▶

Back

Close

Full Screen / Esc

Print Version

Interactive Discussion

Emergence of a linear tracer source from air concentration measurements

J.-P. Issartel

[Title Page](#)[Abstract](#)[Introduction](#)[Conclusions](#)[References](#)[Tables](#)[Figures](#)[⏪](#)[⏩](#)[◀](#)[▶](#)[Back](#)[Close](#)[Full Screen / Esc](#)[Print Version](#)[Interactive Discussion](#)

as carbon dioxide, monoxide or methane is a very different inverse problem involving adjoint techniques (Marchuk, 1964; Tarantola, 1987; Uliasz and Pielke, 1991; Enting et al., 1995; Enting, 2000; Wotawa et al., 2003). At the moment of the measurement the history of the sample is concentrated in the detector. This results in singularities (Ashbaugh et al., 1985; Stohl, 1998; Baklanov, 2000) holding the reconstruction of the source up. This corresponds to the classical problem of data assimilation: how spreading the local information to the whole system (Bouttier and Courtier, 1999). The obstacle compromises the achievement of the natural idea, based on perturbation theory (Gram, 1879; Cheney, 1966; Marchuk, 1973), to use as base functions of the inverse problem the adjoint concentrations of the measurements. The concept of illumination was introduced (Issartel, 2003) to give the singularities a sense. The excessive influence of the neighbourhood of the detectors could be reduced, then, by introducing a weighting function thus changing the effective geometry of the domain. This paper aims at optimising the choice of this function.

To begin with in Sect. 2 the reader is reminded of the definition of the illumination as a quantitative description for the intuitive idea that the various regions of the space time domain are not equally well seen by the measurements. The general inversion strategy is presented. The renormalising or weighting function to be optimised is defined, its geometric meaning is formulated in terms of a scalar product. The influence of the measurement errors will not be dealt with until Sect. 9; the influence of the model errors will be addressed only in the calculations, not in the theory. In Sect. 3 the focus is on the so called background error covariance matrix. The conclusion is that this statistical object is also a geometric scalar product and it also gives indications about which regions are well or badly seen. Unlike the previous one, this product is fuzzy: the parts of the domain are not seen distinctly and separately. In Sect. 4, despite this difficulty, both above products are identified after considering that, in the physical world of observable facts, the part of a source that was not seen by the inversion, somehow, does not exist. The pendent choice of the renormalising function appears then to be a statistical hypothesis not only about the expectable sources but also about the ex-

Emergence of a linear tracer source from air concentration measurements

J.-P. Issartel

Title Page

Abstract

Introduction

Conclusions

References

Tables

Figures

⏪

⏩

◀

▶

Back

Close

Full Screen / Esc

Print Version

Interactive Discussion

pectable values of the measurements now differentiated from the measurement errors. The Sect. 5 is of an other nature. It is noted that the renormalising function and its associated illumination function both can be regarded as weights so that their equality becomes a consistency requirement. The resulting criterion for the choice of the function is shown, by means of unfriendly mathematics, to select one single possibility. The Sect. 6 is a section of interpretation. The above formal criterion is shown to coincide with a hypothesis of best predictability for the values of the measurements. The entropy of their distribution is minimised thus defining a relevant entropy and removing inversion artefacts. In Sect. 7 the notations of the quantum mechanics are introduced to stress the coincidence of the same criterion with the definition of the pure states. The relevance of the pivotal quantum concepts of state and observable is established in Sect. 8. The sources of tracer are just like the wave functions with respect to the states. The influence of measurement errors is described in the Sect. 9. The Sect. 10 is again a section of interpretation with a discussion about the “known domain”. The object is defined and approximate methods are proposed to view it. Finally the strategy is compared in Sects. 11 and 12 to the first ETEX experiment with synthetic and real data. ETEX1 was a twelve hour point release (Brandt et al., 1997; Wendum, 1998; Seibert, 2001) so that it enables to obtain an impulse response of the algorithms. Nevertheless its relevance with respect to a method devoted to widespread sources might be questioned. Hence, the case of an artificial widespread source was included in the calculations. For comparison purpose a series of more traditional inversions with Gaussian base functions was also achieved.

2. Reminder about the illumination

The mixing ratio of an atmospheric tracer in unit amount of tracer per unit mass of air will be denoted $\chi(\mathbf{x})$ with a space-time coordinate $\mathbf{x}=(x, y, z, t)$. In Ω , the atmospheric domain, (x, y) is the horizontal position and z the altitude; t is the date in the time domain T . Under investigation is the source $\sigma(x, y, z, t)=\sigma(\mathbf{x})$ of this tracer in unit amount

Emergence of a linear tracer source from air concentration measurements

J.-P. Issartel

Title Page

Abstract

Introduction

Conclusions

References

Tables

Figures

◀

▶

◀

▶

Back

Close

Full Screen / Esc

Print Version

Interactive Discussion

of tracer per unit mass of air and per unit time. We shall suppose that there is a linear link $\chi = \mathcal{L}(\sigma)$ corresponding to the following dispersion law including a turbulent term $\zeta(\chi)$ and a term for linear creation or killing $\alpha\chi$ describing for instance a radioactive decay with a position dependent scavenging rate $\alpha(\mathbf{x})$. The law must be adequately complemented by zero boundary conditions. The wind is denoted by $\mathbf{v}(\mathbf{x})$:

$$\frac{\partial \chi}{\partial t} + \mathbf{v} \cdot \nabla \chi + \zeta(\chi) + \alpha\chi = \sigma \quad (1)$$

The concentration measurements μ_1, \dots, μ_n used to infer σ may be described in a very symmetric way. To describe the sample number i we need know how much air has been taken where and when; a function $\pi_i(\mathbf{x})$ is introduced:

$$\mu_i = \int_{\Omega \times T} \rho \chi \pi_i(\mathbf{x}) d\mathbf{x} \quad (2)$$

The unit of the π_i is tied to that of the μ_i . Here with the μ_i described as mixing ratios, the π_i will be normalised with respect to the mass of the samples: $\int \rho \pi_i(\mathbf{x}) d\mathbf{x} = 1$. The measurements behave like a scalar product:

$$\mu_i = (\chi, \pi_i) = (\mathcal{L}(\sigma), \pi_i) \quad (\phi, \psi) = \int_{\Omega \times T} \rho \phi \psi d\mathbf{x} \quad (3)$$

By introducing the adjoint operator \mathcal{L}^* and the adjoint concentrations $r_i = \mathcal{L}^*(\pi_i)$ we obtain:

$$\mu_i = \int_{\Omega \times T} \rho \sigma r_i d\mathbf{x} - \frac{\partial r_i}{\partial t} - \mathbf{v} \cdot \nabla r_i + \zeta(r_i) + \alpha r_i = \pi_i \quad (4)$$

The derivation of the adjoint law for r_i is described in (Hourdin and Issartel, 2000; Issartel and Baverel, 2003) with emphasis to the self adjoint nature of ζ in the case of a time-symmetric turbulence; the adjoint law must be complemented by the adjoint boundary conditions which are in fact zero boundary conditions. A linear combination

σ_{\parallel} of the r_i might be proposed as an estimation for σ . The coefficients would be obtained linearly from the measurements after inverting the Gram covariance matrix \mathbf{H} of the r_i :

$$\boldsymbol{\mu} = \begin{bmatrix} \mu_1 \\ \vdots \\ \mu_n \end{bmatrix} \quad \boldsymbol{\lambda} = \begin{bmatrix} \lambda_1 \\ \vdots \\ \lambda_n \end{bmatrix} \quad \mathbf{H} = [h_{i,j}] \quad h_{i,j} = (r_i, r_j) \quad (5)$$

$$\sigma_{\parallel}(\mathbf{x}) = \sum_{i=1}^n \lambda_i r_i(\mathbf{x}) \quad \text{with} \quad \boldsymbol{\lambda} = \mathbf{H}^{-1} \boldsymbol{\mu}$$

5 We shall use as well the following notations:

$$\sigma_{\parallel} = \boldsymbol{\lambda} \cdot \mathbf{r} \quad \mathbf{r}(\mathbf{x}) = \begin{bmatrix} r_1(\mathbf{x}) \\ \vdots \\ r_n(\mathbf{x}) \end{bmatrix} \in \mathbb{R}_+^n \quad (6)$$

$$\sigma_{\parallel} = \boldsymbol{\mu} \cdot \mathbf{g} \quad \mathbf{g}(\mathbf{x}) = \begin{bmatrix} g_1(\mathbf{x}) \\ \vdots \\ g_n(\mathbf{x}) \end{bmatrix} = \mathbf{H}^{-1} \mathbf{r} \in \mathbb{R}^n \quad (7)$$

The families of functions $\{r_1, \dots, r_n\}$ and $\{g_1, \dots, g_n\}$ are dual with the meaning that (δ is Kronecker's symbol):

$$10 \quad (r_i, g_j) = \int_{\Omega \times T} \rho r_i g_j d\mathbf{x} = \delta_{i,j} \quad (8)$$

We noticed in (Issartel, 2003) that this strategy was not well defined. Compared to the atmosphere the samples are very small so that the r_i display peaks by the position of the detectors. Due to the peaks the self interaction coefficients $h_{i,i}$ are very large; they are singular in the theoretical case of Dirac detectors. To remove the obstacle we had to introduce approximations \tilde{r}_i of the retroplumes with arbitrarily large but finite norms

Emergence of a linear tracer source from air concentration measurements

J.-P. Issartel

Title Page

Abstract

Introduction

Conclusions

References

Tables

Figures

◀

▶

◀

▶

Back

Close

Full Screen / Esc

Print Version

Interactive Discussion

$\tilde{h}_{i,j}=(\tilde{r}_j, \tilde{r}_i)$. The failure of the inversion strategy was described in terms of a function of illumination \tilde{E} ; the left superscript t stands for the transposition:

$$\tilde{E}(\mathbf{x}) = {}^t\tilde{r}(\mathbf{x})\tilde{\mathbf{H}}^{-1}\tilde{r}(\mathbf{x}) = {}^t\tilde{r}(\mathbf{x}) \cdot \tilde{g}(\mathbf{x}) \geq 0$$

$$\int_{\Omega \times T} \rho \tilde{E}(\mathbf{x}) d\mathbf{x} = n \quad (9)$$

The second equation is obtained as a trace from the definition (5) of \mathbf{H} or $\tilde{\mathbf{H}}$: $\int \rho f \tilde{\mathbf{H}}^{-1} \tilde{r}^t \tilde{r} d\mathbf{x} dt = \mathbf{I}$; \mathbf{I} is the $n \times n$ identity matrix. The matrix $\tilde{\mathbf{M}}(\mathbf{x}) = f(\mathbf{x}) \tilde{\mathbf{H}}^{-1} \tilde{r}(\mathbf{x}) {}^t\tilde{r}(\mathbf{x})$ is the influence the inversion attributes, per unit mass of ambient air, to \mathbf{x} : the contribution from this point to measurements $\boldsymbol{\mu}$ is estimated as $\rho \tilde{\mathbf{M}}(\mathbf{x}) \boldsymbol{\mu} d\mathbf{x}$. The illumination $\tilde{E}(\mathbf{x})$ is the trace of $\tilde{\mathbf{M}}(\mathbf{x})$ and may accordingly be interpreted as the share of the n available pieces of information attributed to (\mathbf{x}) . For a point seen by no detector $\tilde{E}(\mathbf{x})$ vanishes; on the contrary in the neighbourhood of the detectors $\tilde{E}(\mathbf{x})$ becomes excessively large. This bad geometry is transmitted to the estimate σ_{\parallel} as illustrated by Fig. 2a and c. We proposed to smooth the inversion by introducing a renormalising function $f(\mathbf{x}) \geq 0$ and a new scalar product $(\cdot, \cdot)_f$:

$$(\sigma, \sigma')_f = \int_{\Omega \times T} \rho(\mathbf{x}) f(\mathbf{x}) \sigma(\mathbf{x}) \sigma'(\mathbf{x}) d\mathbf{x} \quad (10)$$

$$\mu_j = \int \rho f \sigma(\mathbf{x}) r_{fj} d\mathbf{x} = (\sigma, r_{fj})_f \quad r_{fj}(\mathbf{x}) = \frac{\tilde{r}_j(\mathbf{x})}{f(\mathbf{x})}$$

The function f was aimed at removing the peaks from the r_{fj} , that are adjoint concentrations in the sense of the new product, and at building a smooth estimate $\sigma_{\parallel f}$:

$$\mathbf{H}_f = [h_{f,i,j}] \quad h_{f,i,j} = (r_{fi}, r_{fj})_f = \int_{\Omega \times T} \rho \frac{\tilde{r}_i \tilde{r}_j}{f} d\mathbf{x}$$

$$\boldsymbol{\lambda}_f = \mathbf{H}_f^{-1} \boldsymbol{\mu} \quad \sigma_{\parallel f}(\mathbf{x}) = \boldsymbol{\lambda}_f \cdot \mathbf{r}_f(\mathbf{x}) \quad (11)$$

Emergence of a linear tracer source from air concentration measurements

J.-P. Issartel

Title Page

Abstract

Introduction

Conclusions

References

Tables

Figures

⏪

⏩

◀

▶

Back

Close

Full Screen / Esc

Print Version

Interactive Discussion

Emergence of a linear tracer source from air concentration measurements

J.-P. Issartel

Title Page

Abstract

Introduction

Conclusions

References

Tables

Figures

⏪

⏩

◀

▶

Back

Close

Full Screen / Esc

Print Version

Interactive Discussion

The inversion was clearly improved for the following empirical choice
 $f(\mathbf{x}) = \max \left[\tilde{E}(\mathbf{x}), \frac{\tilde{E}_{max}}{1000} \right]$ inferred from the observation that around the detectors
 the illumination \tilde{E} decreased a factor 1000 from its maximum value for irrelevant space
 scales. The aim of the present paper is to put the choice of the renormalising function
 on non empirical bases.

The source of a pollutant emitted at the surface Σ of the ground or oceans may be
 described as a release $\sigma_s(x, y, t)$ at the altitude $z_s(x, y)$ in unit amount of tracer per
 unit area and time. The measurements become:

$$\mu_i = \int_{\Sigma \times T} \sigma_s(x, y, t) r_i(x, y, z_s, t) dx dy dt \quad (12)$$

This source will be investigated as a combination of the restrictions
 $r_{s,i}(x, y, t) = r_i(x, y, z_s, t)$ with a renormalisation of the domain $\Sigma \times T$.

3. Geometry and statistics

The following discussion is the basis of the transformation, illustrated on Fig. 3, of the
 illumination into a curved geometry. Before addressing the optimal choice of the renor-
 malising function f it is preferable to investigate some properties tied to its introduction.
 Under investigation in this section and the following one are the effects on the quality
 of the estimate of the geometric properties of the measurements and of the inversion
 independently of any measurement errors. The effect of measurement errors will be
 addressed in Sect. 9. The effect of model errors will be addressed only through the
 calculations, not in theoretical terms. Obviously the function f with the product $(\cdot)_f$
 are geometric objects. The statistical aspects are less visible. Keys will stem from
 the careful consideration of the usual equations of data assimilation. The method is
 traditionally presented in a discretised form with a finite number ν_{max} of meshes at
 mean space-time positions \mathbf{x}^v of space-time weights d^v (corresponding to the integral

element $\rho d\mathbf{x}$). We keep the same notation σ for the continuous source $\sigma(\mathbf{x})$ and the corresponding column vector integrated in each mesh with elements: $\sigma_v = d^v \sigma(\mathbf{x}^v)$.

The inversion of μ_1, \dots, μ_n is usually addressed with a functional \mathcal{J} : the estimate σ_{est} of the unknown real source σ is the source s minimising $\mathcal{J}(s)$. The meaning of \mathbf{B} , \mathbf{R} and \mathbf{Q} is explained below:

$$\mathcal{J}(s) = {}^t s \mathbf{B}^{-1} s + {}^t (\mathbf{R}s - \boldsymbol{\mu}) \mathbf{Q}^{-1} (\mathbf{R}s - \boldsymbol{\mu}) \quad (13)$$

Most often σ is intended in fact as the mismatch between the sought source and an a priori estimate. The $v_{\max} \times v_{\max}$ matrix \mathbf{B} is the covariance matrix of the estimation error or background error: $\mathbf{B} = \overline{\sigma \sigma^t}$. The bar stands for the statistical expectation. Correspondingly $\boldsymbol{\mu} = \mathbf{R}\sigma + \delta\boldsymbol{\mu}$ is the mismatch between the measurements really observed and the values synthesised for σ_{pri} by the available model. The $n \times v_{\max}$ matrix \mathbf{R} stands for the observation operator, or rather, the linear or linearised deterministic part of the observation operator; the lines of \mathbf{R} correspond to our r_i . The $n \times n$ covariance matrix \mathbf{Q} of the measurement errors describes the imperfections of the observations and model: $\mathbf{Q} = \overline{\delta\boldsymbol{\mu} \delta\boldsymbol{\mu}^t}$. The paper is not about measurement errors, skipping them from Eq. (13) amounts to taking an infinite \mathbf{Q}^{-1} and to minimising ${}^t s \mathbf{B}^{-1} s$ under the constraints that s strictly obeys the measurements, $\mathbf{R}s = \boldsymbol{\mu}$.

In the present context there is no explicit a priori estimate. It is possible to consider that the null source plays this role. Accordingly, $\mathbf{B} = \overline{\sigma \sigma^t}$ may be seen as the covariance matrix of the source investigated by the measurements.

The expression ${}^t s \mathbf{B}^{-1} s$ shows that the description of the estimation errors may be formulated by introducing a specific scalar product $\langle \phi, \psi \rangle_k = {}^t \phi \mathbf{B}^{-1} \psi$. The label “k” means that this product gives a geometric account of our knowledge and lack of knowledge. In the continuous case $\langle \cdot, \cdot \rangle_k$ would be described by a kernel b^- : $\langle \phi, \psi \rangle_k = \int \phi(\mathbf{x}) b^-(\mathbf{x}, \mathbf{y}) \psi(\mathbf{y}) d\mathbf{x} d\mathbf{y}$. The diagonal elements of the discretised matrix \mathbf{B} are, by definition, $b_{v,v} = \overline{\sigma_v^2} = (d^v \sigma(\mathbf{x}^v))^2$. If \mathbf{B} was diagonal so would be \mathbf{B}^{-1} with elements $\frac{1}{b_v}$. In the geometry of a diagonal \mathbf{B}^{-1} the weights d^v of the meshes would be

Emergence of a linear tracer source from air concentration measurements

J.-P. Issartel

Title Page

Abstract

Introduction

Conclusions

References

Tables

Figures

⏪

⏩

◀

▶

Back

Close

Full Screen / Esc

Print Version

Interactive Discussion

replaced by $\frac{d^v}{\sqrt{b_v}}$ and the source would be discretised as $\sigma'_v = \frac{d^v \sigma(x^v)}{\sqrt{b_v}}$ with a covariance $\overline{\sigma'_v{}^2} = 1$. This diagonal example shows that \mathbf{B}^{-1} transforms the subspace $\Omega \times T$ of \mathbb{R}^4 into a curved space in which the information is equally distributed. Hence we shall say that $\Omega \times T$ endowed with the product $\langle \cdot, \cdot \rangle_k$ is a version of the known domain.

5 The non vanishing off diagonal terms $b_{v,v'}^-$ of \mathbf{B}^{-1} indicate a degree of confusion between the meshes v and v' that cannot be totally distinguished. When \mathbf{B}^{-1} or the kernel b^- are purely diagonal the known domain will be called “separate”.

The strategy proposed in the previous section amounts to minimising the norm $(s, s)_f = \int \rho f s^2 dx dt$ under the constraints that s strictly obeys the measurements, $(s, r_{fi})_f = \mu_i$. It may then be suspected that the choice of a function f is somehow a hypothesis about the form of \mathbf{B} (in fact \mathbf{B}^{-1}) and $\langle \cdot, \cdot \rangle_k$. The renormalising function may be represented by a diagonal matrix:

$$\mathbf{F} = \begin{bmatrix} f^1 & & \\ & \ddots & \\ & & f^{v_{\max}} \end{bmatrix} \quad (14)$$

15 The straightforward link $\mathbf{B} = \mathbf{F}^{-1}$ or $\langle \cdot, \cdot \rangle_k = \langle \cdot, \cdot \rangle_f$ is hardly acceptable. It would imply a separate geometry of the observed domain with vanishing correlations $\overline{\sigma(x)\sigma(y)} = 0$ unless $\mathbf{x} = \mathbf{y}$. This obstacle will be understood and arranged in Sect. 4. We shall show that, as far as no other information than the measurements is available, $\langle \cdot, \cdot \rangle_f$ is physically equivalent to a non separate product $\langle \cdot, \cdot \rangle_k$ which is a more reasonable candidate for the identification with $\langle \cdot, \cdot \rangle_k$.

20 Before exploring the relationship between \mathbf{B} and \mathbf{F} in the next section two points must be stressed. Firstly the definition of \mathbf{B} with the kernel $b(\mathbf{x}, \mathbf{y}) = \overline{\sigma(\mathbf{x})\sigma(\mathbf{y})}$ explicitly refers to some probability distribution among the possible sources σ . No such statistical hypothesis is contained in the definition of \mathbf{F} . A link between both objects must be seen, accordingly, not as a mathematically necessary requirement but rather as a physically

Emergence of a linear tracer source from air concentration measurements

J.-P. Issartel

Title Page

Abstract

Introduction

Conclusions

References

Tables

Figures

⏪

⏩

◀

▶

Back

Close

Full Screen / Esc

Print Version

Interactive Discussion

Emergence of a linear tracer source from air concentration measurements

J.-P. Issartel

Title Page

Abstract

Introduction

Conclusions

References

Tables

Figures

◀

▶

◀

▶

Back

Close

Full Screen / Esc

Print Version

Interactive Discussion

motivated hypothesis. The link will imply a hypothesis about the probability distribution of the source under investigation by means of the measurements. Secondly, as already mentioned, the quality of the estimate is not investigated yet in terms of measurement errors but in terms of the geometry of the physical system. The effect of the errors will be considered later in Sect. 9.

4. An assumption

σ may always be decomposed as $\sigma = \sigma_{\parallel f} + \sigma_{\perp f}$ into its parts parallel and orthogonal to the $r_{f,i}$:

$$\overline{\sigma(\mathbf{x})\sigma(\mathbf{y})} = \overline{\sigma_{\parallel f}(\mathbf{x})\sigma_{\parallel f}(\mathbf{y})} + \overline{\sigma_{\parallel f}(\mathbf{x})\sigma_{\perp f}(\mathbf{y})} + \overline{\sigma_{\perp f}(\mathbf{x})\sigma_{\parallel f}(\mathbf{y})} + \overline{\sigma_{\perp f}(\mathbf{x})\sigma_{\perp f}(\mathbf{y})} \quad (15)$$

with:

$$\overline{\sigma_{\parallel f}(\mathbf{x})\sigma_{\parallel f}(\mathbf{y})} = \mathbf{r}_f(\mathbf{x}) \mathbf{H}_f^{-1} \overline{\boldsymbol{\mu}^t \boldsymbol{\mu}} \mathbf{H}_f^{-1} \mathbf{r}_f(\mathbf{y}) \quad (16)$$

The last expression contains the measurement (or mismatch) covariance matrix $\overline{\boldsymbol{\mu}^t \boldsymbol{\mu}}$ that is distinguished in the present development from $\mathbf{Q} = \delta \boldsymbol{\mu}^t \delta \boldsymbol{\mu}$. If the information available from the measurements is optimally used in restoring $\sigma_{\parallel f}$ it is consistent to consider that $\sigma_{\perp f}$ is essentially unknown and undetermined. Then, the terms in the second line of Eq. (15) always vanish and also the term in the third line when $\mathbf{x} \neq \mathbf{y}$.

When $\mathbf{x} = \mathbf{y}$ the quantity $\overline{\sigma_{\perp f}(\mathbf{x})^2}$ is non negative but undetermined.

This conclusion may surprise because the evaluation of \mathbf{B} is generally addressed in terms of indirect observations of an error $\delta\sigma = \sigma - \sigma_{est}$ corresponding here to $\sigma_{\perp f} = \sigma - \sigma_{\parallel f}$. The present reasoning does not invoke such additional information. It just states that the questions to be answered are: which regions are well seen? which ones are

Emergence of a linear tracer source from air concentration measurements

J.-P. Issartel

poorly seen? which confusions are possible between a source here and a source there?

The Eqs. (15) and (16) have an even stranger consequence. The assumption that $b(\mathbf{x}, \mathbf{y}) = \sigma(\mathbf{x})\sigma(\mathbf{y})$ is a continuous function, combined with the continuity of Eq. (16), implies that $\sigma_{\perp f}(\mathbf{x})^2$ must vanish as well. We think this just means that $\sigma_{\perp f}(\mathbf{x})^2$ is not a relevant physical object. It is clear indeed that, from a purely mathematical point of view that, if the subspace of the sources parallel to the r_{fi} is well defined, the subspace of the perpendicular sources cannot be defined in a unique unambiguous way. A more physical point of view may be obtained by decomposing $(\cdot)_f$ as:

$$(\sigma, \sigma)_f = (\sigma_{\parallel f}, \sigma_{\parallel f})_f + (\sigma_{\perp f}, \sigma_{\perp f})_f \quad (17)$$

The only term of this expression that may be known and used in practice is $(\sigma_{\parallel f}, \sigma_{\parallel f})_f$. The term $(\sigma_{\perp f}, \sigma_{\perp f})_f$ is not knowable so that its physical status may be questioned, which is equivalent to question the status of $\sigma_{\perp f}(\mathbf{x})^2$. Let's denote:

$$\langle \sigma, \sigma \rangle_f = (\sigma_{\parallel f}, \sigma_{\parallel f})_f \quad (18)$$

This is still a scalar product of σ because $\sigma_{\parallel f} = \mathbf{P}\sigma$ is a linear function of σ . Denoted in matrix form, \mathbf{P} is an orthogonal projector, in the sense of $(\cdot)_f$, on the space spanned by the r_{fi} : it is self adjoint and $\mathbf{P}^2 = \mathbf{P}$. The continuous form of \mathbf{P} may be obtained by putting the form (10) of $\boldsymbol{\mu}$ into the expression (11) of $\sigma_{\parallel f}$:

$$\sigma_{\parallel f}(\mathbf{x}) = \int_{\Omega \times \mathcal{T}} \sigma(\mathbf{y}) f(\mathbf{y}) {}^t r_f(\mathbf{y}) \mathbf{H}_f^{-1} r_f(\mathbf{x}) \rho(\mathbf{y}) d\mathbf{y} \quad (19)$$

If σ' is another source we substitute two such expressions as Eq. (19) into the definition (10) of $(\sigma_{\parallel f}, \sigma'_{\parallel f})_f$. The following expression is obtained for $\langle \cdot, \cdot \rangle_f$ after the simplification of a matrix term $\int r_f(\mathbf{x}) {}^t r_f(\mathbf{x}) d\mathbf{x} = \mathbf{H}_f$:

$$\langle \sigma, \sigma' \rangle_f = \iint \sigma(\mathbf{x}) f(\mathbf{x}) {}^t r_f(\mathbf{x}) \mathbf{H}_f^{-1} r_f(\mathbf{y}) f(\mathbf{y}) \sigma(\mathbf{y}) \rho(\mathbf{x}) d\mathbf{x} \rho(\mathbf{y}) d\mathbf{y} \quad (20)$$

Title Page

Abstract

Introduction

Conclusions

References

Tables

Figures

◀

▶

◀

▶

Back

Close

Full Screen / Esc

Print Version

Interactive Discussion

We think that, despite their mathematical difference, $(\cdot)_f$ and $\langle \cdot \rangle_f$ are physically equivalent with restrictions explained at the end of Sect. 6. In particular the measurements are obtained in the same way with both products:

$$\mu_j = (\sigma, r_{fi})_f = \langle \sigma, r_{fi} \rangle_f \quad (21)$$

- 5 The matrix associated to $(\cdot)_f$ is \mathbf{F} , that tied to $\langle \cdot \rangle_f$ is $\mathbf{PFP}=\mathbf{PF}=\mathbf{FP}$. This is no longer a full rank diagonal matrix so that $\langle \cdot \rangle_f$ is not a separate product. The following identification becomes conceivable:

$$\langle \cdot \rangle_f = \langle \cdot \rangle_k \quad \text{or} \quad \mathbf{B}^{-1} = \mathbf{PF} = \mathbf{FP} \quad (22)$$

10 As stressed in Sect. 3 this relation cannot be demonstrated and must be admitted as a definition or as an assumption. We think the arguments developed in this section and the previous one have made this assumption reasonable. Its interest should now be confirmed by the consequences that will be investigated in the next sections. In fact the Eq. (22) just formulates a link between the statistical description of the sources and the geometric description of the space with a renormalising function f . The assumption

15 is not so big because f is still to be chosen. The choice may be now regarded as a problem of joint optimisation for the geometric and statistical description of the system.

According to Eq. (22) the rank of \mathbf{B}^{-1} , bounded by the number of measurements, is not full. The inverse notation might be questioned but there will be no problem as long as the very working space is that spanned by the r_{fi} .

- 20 The assumption (22) has an important consequence consistent with the intuition. The kernel ρ associated to \mathbf{P} may be read on the Eq. (19):

$$\rho(\mathbf{x}, \mathbf{y}) = f(\mathbf{y}) {}^t r_f(\mathbf{y}) \mathbf{H}_f^{-1} r_f(\mathbf{x}) \quad (23)$$

As $\mathbf{B}^{-1}=\mathbf{PF}$ or $\mathbf{B}=\mathbf{F}^{-1}\mathbf{P}$ we obtain for b the expression:

$$b(\mathbf{x}, \mathbf{y}) = {}^t r_f(\mathbf{y}) \mathbf{H}_f^{-1} r_f(\mathbf{x}) \quad (24)$$

Emergence of a linear tracer source from air concentration measurements

J.-P. Issartel

Title Page

Abstract

Introduction

Conclusions

References

Tables

Figures

◀

▶

◀

▶

Back

Close

Full Screen / Esc

Print Version

Interactive Discussion

The following alternative expression for $b(\mathbf{x}, \mathbf{y}) = \overline{\sigma(\mathbf{x})\sigma(\mathbf{y})}$, deduced from the Eq. (16), was justified above:

$$\overline{\sigma(\mathbf{x})\sigma(\mathbf{y})} = \mathbf{r}_f(\mathbf{x}) \mathbf{H}_f^{-1} \overline{\boldsymbol{\mu}^t \boldsymbol{\mu}} \mathbf{H}_f^{-1} \mathbf{r}_f(\mathbf{y}) \quad (25)$$

Hence the expectable values of the measurements, called here “anticipations”, obey an a priori distribution law with a covariance matrix:

$$\overline{\boldsymbol{\mu}^t \boldsymbol{\mu}} = \mathbf{H}_f \quad \text{or} \quad \overline{\mu_i \mu_j} = (r_{fi}, r_{fj})_f = \langle r_{fi}, r_{fj} \rangle_f \quad (26)$$

In particular if two detectors have adjoint functions r_{fi}, r_{fj} that do not overlap, the correlation between the expectable measurements vanish: $\overline{\mu_i \mu_j} = 0$. For the continuation the Eq. (22) will be complemented by the assumption that the measurement anticipations follow a Gaussian law with a covariance matrix $\overline{\boldsymbol{\mu}^t \boldsymbol{\mu}} = \mathbf{H}_f$.

It is finally important to stress that the r_i were initially defined as the functions adjoint to the measurements according to the ordinary geometry. When the renormalising function f was introduced the r_{fi} have been defined as the functions adjoint to the measurements for the product $(\cdot)_f$. Now the same r_{fi} may be regarded as functions adjoint through the products $\langle \cdot \rangle_f = \langle \cdot \rangle_k$ describing the geometry and statistics of the system.

5. Formal consistency

The function f was introduced based on the idea that a weight should be attributed to each part of the space time domain in order to interpret the measurements. The purpose of this section is to show that this idea is consistent with one single function f . This function is characterised by the Eq. (29) and may be easily calculated by the algorithm (35). As this section is mainly technical, the reader not interested in the mathematical details may consider just these results and go directly to the Sect. (6) where a physical interpretation will be proposed.

Emergence of a linear tracer source from air concentration measurements

J.-P. Issartel

Title Page

Abstract

Introduction

Conclusions

References

Tables

Figures

◀

▶

◀

▶

Back

Close

Full Screen / Esc

Print Version

Interactive Discussion

Emergence of a linear tracer source from air concentration measurements

J.-P. Issartel

Title Page

Abstract

Introduction

Conclusions

References

Tables

Figures

◀

▶

◀

▶

Back

Close

Full Screen / Esc

Print Version

Interactive Discussion

The choice of the renormalising function is subject to decisive constraints coming logically with the working hypotheses. Firstly $f(\mathbf{x})$ may be regarded as a distribution of geometric weights to the various parts of $\Omega \times T$. The optimisation should be performed among functions of a given total weight. All choices of the fixed total weight are equal in principle but the consistency of the forthcoming development is clearer if the constant is taken to be n , the number of pieces of information. So the optimal f will be defined among the functions obeying:

$$r(\mathbf{x}) \neq 0 \implies f(\mathbf{x}) > 0 \text{ and } \int_{\Omega \times T} \rho f d\mathbf{x} = n \quad (27)$$

To f and its scalar product may be associated a renormalised illumination E_f . The second equation, like Eq. (9), is the trace of the identity \mathbf{I} :

$$\int_{\Omega \times T} \rho f {}^t r_f(\mathbf{x}) \mathbf{H}_f^{-1} r_f(\mathbf{x}) d\mathbf{x} = n \quad (28)$$

$$E_f(\mathbf{x}) = f(\mathbf{x}) {}^t r_f(\mathbf{x}) \mathbf{H}_f^{-1} r_f(\mathbf{x})$$

Now again $E_f(\mathbf{x}, t)$ appears to be a weight attributed to (\mathbf{x}, t) by the inversion and it obeys the constraints (27). The consistency of the weighting strategy requires that $E_f = f$. Hence f should be chosen in such a way that:

$$r(\mathbf{x}) \neq 0 \implies {}^t r_f(\mathbf{x}) \mathbf{H}_f^{-1} r_f(\mathbf{x}) = 1 \quad (29)$$

In fact the conditions (27) and (29) are satisfied by one single function f . To see that we must make a detour with the function $\det \mathbf{H}_f$. Note that this section develops the arguments from a purely technical point of view but of course, in the following sections, the objects will receive a physical interpretation. The function $\det \mathbf{H}_f$ reaches its minimum for exactly one function f among those obeying (27) because it is strictly concave. Still because it is concave, the local optimality conditions become global and these conditions are exactly (29).

Emergence of a linear tracer source from air concentration measurements

J.-P. Issartel

Title Page	
Abstract	Introduction
Conclusions	References
Tables	Figures
◀	▶
◀	▶
Back	Close
Full Screen / Esc	

Print Version
Interactive Discussion

Let's discretise the domain $\Omega \times T$ into a number v_{\max} of meshes, like in Sects. 3 and 4, with now the following notations: (x^v) and d^v are the space-time position and space-time mass (the mass multiplied by the duration) of the meshes, $r_i^v = \tilde{r}_i(x^v)$, $f^v = f(x^v)$, $r_{f,i}^v = \frac{\tilde{r}_i(x^v)}{f(x^v)}$ etc. The discretisation can be made as thin as possible so that the results are valid for the continuous problem. With these notations the matrix H_f may be written:

$$H_f = \tag{30}$$

$$\begin{bmatrix} d^1 \frac{r_1^1 r_1^1}{f^1} + d^2 \frac{r_1^2 r_1^2}{f^2} + \dots, & d^1 \frac{r_1^1 r_2^1}{f^1} + d^2 \frac{r_1^2 r_2^2}{f^2} + \dots, & \dots, & \dots \\ d^1 \frac{r_2^1 r_1^1}{f^1} + d^2 \frac{r_2^2 r_1^2}{f^2} + \dots, & d^1 \frac{r_2^1 r_2^1}{f^1} + d^2 \frac{r_2^2 r_2^2}{f^2} + \dots, & \dots, & \dots \\ d^1 \frac{r_3^1 r_1^1}{f^1} + d^2 \frac{r_3^2 r_1^2}{f^2} + \dots, & d^1 \frac{r_3^1 r_2^1}{f^1} + d^2 \frac{r_3^2 r_2^2}{f^2} + \dots, & \dots, & \dots \\ \dots & \dots & \dots & \dots \end{bmatrix}$$

The columns of H_f decompose into a sum of subcolumns corresponding to the contributions from the meshes, each bearing a factor $\frac{1}{f^v}$. After accurate considerations about the linear dependence of the subcolumns appearing in the various columns, the following expression is developed by means of the n -linearity of the determinant; G stands for the Gram matrix of a family of n vectors:

$$\det H_f = \sum_{1 \leq v_1 < \dots < v_n \leq v_{\max}} \frac{\det G(r^{v_1}, \dots, r^{v_n})}{f^{v_1} \dots f^{v_n}} \tag{31}$$

$$G = [g_{i,j}] \quad g_{i,j}(r^{v_i}, \dots, r^{v_j}) = {}^t \tilde{r}(x^{v_i}) \cdot \tilde{r}(x^{v_j})$$

A Gram determinant is strictly positive except when some r^v vanishes. Accordingly, as far as we consider only the meshes effectively observed by one or more detectors, $\det H_f$ is a strictly concave function of f because each term $1/f^{v_1} \dots f^{v_n}$ is. As f is constrained by (27) to a compact set, $\det H_f$ reaches a minimum. The latter is characterised by its first order insensitiveness to variations δf preserving the total weight: $\sum_{v=1}^{v_{\max}} d^v \delta f^v = 0$.

Emergence of a linear tracer source from air concentration measurements

J.-P. Issartel

Title Page

Abstract

Introduction

Conclusions

References

Tables

Figures

⏪

⏩

◀

▶

Back

Close

Full Screen / Esc

Print Version

Interactive Discussion

The variation of $\mathbf{H}^{f+\delta f} = \mathbf{H}_f + \delta \mathbf{H}$ due to δf is obtained by means of the Eq. (30) with the identities $\frac{1}{f^v + \delta f^v} \simeq \frac{1}{f^v} - \frac{\delta f^v}{f^v f^v}$ and $\frac{r^{vk}}{f^v} = r_f^{vk}$:

$$\delta h_{f,i,j} = -\delta f^1 d^1 r_{fi}^1 r_{fj}^1 - \delta f^2 d^2 r_{fi}^2 r_{fj}^2 - \dots$$

$$\delta \mathbf{H}_f = - \sum_{\nu=1}^{v_{\max}} d^\nu f^\nu r_f(x^\nu) {}^t r_f(x^\nu) \quad (32)$$

5 It is well known that $\det(\mathbf{H}_f + \delta \mathbf{H}) \simeq \det \mathbf{H}_f + \text{tr}(\mathbf{H}_f^{-1} \delta \mathbf{H})$ and it is easily seen that for any two vectors \mathbf{a} , \mathbf{b} we have: $\text{tr}(\mathbf{H}_f^{-1} \mathbf{a} {}^t \mathbf{b}) = {}^t \mathbf{b} \mathbf{H}_f^{-1} \mathbf{a}$. This leads finally to the following result:

$$\delta \det \mathbf{H}_f = - \sum_{\nu=1}^{v_{\max}} d^\nu \delta f^\nu {}^t r_f(x^\nu) \mathbf{H}_f^{-1} r_f(x^\nu) \quad (33)$$

This variation vanishes for all admissible δf if and only if the ${}^t r_f(x^\nu) \mathbf{H}_f^{-1} r_f(x^\nu)$ are all equal. This is indeed the constraint (29).

10 It is rather easy to numerically obtain f subject to (27) and (29). An iterative procedure may be initiated with $f_0(\mathbf{x}) \equiv 1$; this function is positive but obeys neither (27) nor (29). At each iteration:

$$\int_{\Omega \times \mathbb{T}} \rho f_k {}^t r_{f_k} \mathbf{H}_{f_k}^{-1} r_{f_k} d\mathbf{x} = n \quad k \geq 1 \quad (34)$$

15 The iterations are defined by:

$$f_{k+1}(\mathbf{x}) = f_k(\mathbf{x}) \sqrt{{}^t r_{f_k}(\mathbf{x}) \mathbf{H}_{f_k}^{-1} r_{f_k}(\mathbf{x})} \quad (35)$$

As ${}^t r_{f_k} \mathbf{H}_{f_k}^{-1} r_{f_k}$ tends rapidly to 1 the condition (29) is fulfilled; the condition (27) is also fulfilled as a limit of the Eq. (34). After nine iterations we already have $0.985 \leq {}^t r_{f_9} \mathbf{H}_{f_9}^{-1} r_{f_9} \leq 0.995$.

6. Intrinsically relevant information

The entropy associated to an experiment with N discrete possibilities having probabilities p_i was formulated by [Hartley \(1928\)](#); [Shannon \(1948\)](#) after the work of Boltzmann in statistical thermodynamics:

$$S = - \sum_{i=1}^N p_i \log p_i \quad (36)$$

The quantity $-\log p_i$ is a measure of the information got by an observer discovering the result number i ; it may be thought of as the surprise of the observer, weak for very probable events with $p_i \simeq 1$, and strong for improbable events. The entropy of information (36) is the expectation of this information and as such it is a measure of the relevance of the experiment.

If the outcome of the experiment is a discrete vector $\boldsymbol{\mu}$ with a probability distribution function $p(\boldsymbol{\mu})$ the entropy of information is generalised as:

$$S = - \int p(\boldsymbol{\mu}) \log p(\boldsymbol{\mu}) d\boldsymbol{\mu} \quad (37)$$

This generalisation is not as straightforward as it looks like. An account of the problems may be found in ([Hatori, 1958](#); [Middleton, 1960](#)). The entropy of a continuous Gaussian distribution for μ_1, \dots, μ_n with a covariance matrix \mathbf{H}_f is:

$$p(\boldsymbol{\mu}) = \frac{e^{-\frac{1}{2}\{\boldsymbol{\mu}^t \mathbf{H}_f^{-1} \boldsymbol{\mu}\}}}{\sqrt{(2\pi)^n \det \mathbf{H}_f}} \quad (38)$$

$$S_f = \frac{n}{2} \log(2\pi) + \frac{1}{2} \log \det \mathbf{H}_f$$

Thus the optimal renormalising function f is the one for which the probability distribution of the measurements has the least entropy. Indeed it was shown in the previous section that this optimum minimises $\det \mathbf{H}_f$ for a fixed total weight of f . In other words, the

Emergence of a linear tracer source from air concentration measurements

J.-P. Issartel

Title Page

Abstract

Introduction

Conclusions

References

Tables

Figures

⏪

⏩

◀

▶

Back

Close

Full Screen / Esc

Print Version

Interactive Discussion

Emergence of a linear tracer source from air concentration measurements

J.-P. Issartel

Title Page

Abstract

Introduction

Conclusions

References

Tables

Figures

◀

▶

◀

▶

Back

Close

Full Screen / Esc

Print Version

Interactive Discussion

best geometry for $\Omega \times T$ is the one for which the average information expected from the measurements is reduced to an intrinsic minimum. The entropy S_1 tied to the standard geometry, $f \equiv 1$, is indefinitely large: the measurements, attributed to the close environment of the detectors, become pairwise independent, the off diagonal terms $h_{i,j}$ of the covariance matrix \mathbf{H} vanish while the diagonal terms $h_{i,i}$ diverge. As a result, the source is rebuilt with artefacts evoking some artificial information. The releases focused around the detectors on the Figs. 2a and c, are obviously artefacts. The excess of the entropy S_f tied to some f , compared to the minimum value $S_{f_{opt}}$, may be seen as a measure of this artificial irrelevant information. This entropic excess is a measure of our excessive surprise at discovering the sources of the Figs. 2a and c. When the geometry is optimised the potential sources away from all the detectors are better taken into account.

Let's consider now two situations. In the first situation n measurements μ_1, \dots, μ_n are performed. In the second situation, exactly the same measurements are performed plus one, μ_{n+1} . Note that the subscript $n+1$ is not a chronological indication that this additional measurement is done after the other ones, it is just one more measurement. So, the first situation will correspond to an optimal renormalising function f_n and the statistics of the measurements will follow a $n \times n$ covariance matrix \mathbf{H}_n . In the second case an optimal renormalising function f_{n+1} will be obtained with a $(n+1) \times (n+1)$ covariance matrix \mathbf{H}_{n+1} :

$$\mathbf{H}_n = [h_{n,i,j}] \quad i = 1, \dots, n \quad j = 1, \dots, n$$

$$h_{n,i,j} = \overline{\mu_i \mu_j} / \rho^n = \int_{\Omega \times T} \rho \frac{\tilde{r}_i \tilde{r}_j}{f_n} d\mathbf{x} \quad (39)$$

$$\mathbf{H}_{n+1} = [h_{n+1,i,j}] \quad i = 1, \dots, n+1 \quad j = 1, \dots, n+1$$

$$h_{n+1,i,j} = \overline{\mu_i \mu_j} / \rho^{n+1} = \int_{\Omega \times T} \rho \frac{\tilde{r}_i \tilde{r}_j}{f_{n+1}} d\mathbf{x} \quad (40)$$

Emergence of a linear tracer source from air concentration measurements

J.-P. Issartel

Title Page

Abstract

Introduction

Conclusions

References

Tables

Figures

◀

▶

◀

▶

Back

Close

Full Screen / Esc

Print Version

Interactive Discussion

The bars for the statistical expectation now bear an indication of the situation under examination. There is no reason why f_n and f_{n+1} should be equal. Thus \mathbf{H}_n does not coincide with the $n \times n$ upper diagonal submatrix $\mathbf{H}_{n+1/n}$ of \mathbf{H}_{n+1} . The mere existence of μ_{n+1} changes the statistics of μ_1, \dots, μ_n . This is at first sight a strange result. We could indeed imagine that we perform the additional measurement but do not look at the result. This is of course an effect of how the additional $\tilde{r}_{n+1}(\mathbf{x})$ will overlap with the other $\tilde{r}_i(\mathbf{x})$ thus altering the system of weights distributed in $\Omega \times T$. Despite a first surprise, we can recognise that the fact belongs to the all day life. Our expectations with respect to future events, and accordingly our attitudes, are changed after a school or medical examination, even before the result is known to us or to anybody else. The world with or without the examination is not the same.

Note that if $\tilde{r}_{n+1}(\mathbf{x})$ did not overlap at all with any of the $\tilde{r}_i(\mathbf{x})$, $i \leq n$, then the optimisation of f_{n+1} would split into two separate optimal problems for the domains of $\tilde{r}_{n+1}(\mathbf{x})$ on the one hand, of the other $\tilde{r}_i(\mathbf{x})$ on the other hand. And then the identity $\mathbf{H}_n = \mathbf{H}_{n+1/n}$ would stand. In the reality, two retroplumes always overlap in an early enough past.

The norm of a source was seen to decompose as:

$$(\sigma, \sigma)_f = \int \rho f \sigma^2 d\mathbf{x} = \langle \sigma, \sigma \rangle_f + (\sigma_{\perp}, \sigma_{\perp})_f \quad (41)$$

$$\langle \sigma, \sigma \rangle_f = (\sigma_{\parallel f}, \sigma_{\parallel f})_f$$

Indirectly $(\sigma, \sigma)_f$ is a measure of the amount of tracer released but not only. The total release may even vanish if the positive and negative contributions compensate. Thus $(\sigma, \sigma)_f$ is also a measure of the structural complexity of the source. The part of this complexity that may be captured by the detectors is $\langle \sigma, \sigma \rangle_f \leq (\sigma, \sigma)_f$. From the point of view of the detectors handled with the geometry of $(\cdot, \cdot)_f$, $\sigma_{\parallel f}$ is σ and $\langle \cdot, \cdot \rangle_f$ is $(\cdot, \cdot)_f$. Nevertheless the theoretician often puts himself in the situation to know more about a source than the information available from the measurements. For him $(\cdot, \cdot)_f$ and $\langle \cdot, \cdot \rangle_f$ are different objects. For instance we know the ETEX release but we pretend in our calculations that we know only a few measurements. We propose to use in this situ-

Emergence of a linear tracer source from air concentration measurements

J.-P. Issartel

Title Page

Abstract

Introduction

Conclusions

References

Tables

Figures

⏪

⏩

◀

▶

Back

Close

Full Screen / Esc

Print Version

Interactive Discussion

© EGU 2004

ation the following wording. The quadratic form $(\sigma, \sigma)_f$ will be called the informational energy of the source σ and we shall say that $\langle \sigma, \sigma \rangle_f = (\sigma_{\parallel f}, \sigma_{\parallel f})_f$ is the part of this energy captured by or interacting with the detectors. Then $f(\mathbf{x})\sigma(\mathbf{x})^2$ will be the density of energy per unit mass around the space time position \mathbf{x} in the ordinary geometry where the elementary mass is $\rho d\mathbf{x}$. In the renormalised geometry, the element is $\rho f d\mathbf{x}$ and the density of informational energy around \mathbf{x} is simply $\sigma(\mathbf{x})^2$.

7. New notations

From now on the renormalising function f is supposed to coincide with the optimum characterised in Sect. 5. The following notations will be convenient in which may be recognised the ways of quantum theory as will be later justified by the Eq. (47). To any source σ , producing measurements $\boldsymbol{\mu}$, and any position \mathbf{x} we associate the following line and column vectors defined in \mathbb{R}^n and, as explained with Eq. (47), in its unit sphere \mathbb{S}^n :

$$\langle \sigma | = {}^t \boldsymbol{\mu} \sqrt{\mathbf{H}_f^{-1}} \quad | \sigma \rangle = \sqrt{\mathbf{H}_f^{-1}} \boldsymbol{\mu} \in \mathbb{R}^n \quad (42)$$

$$\langle \mathbf{x} | = {}^t r_f(\mathbf{x}) \sqrt{\mathbf{H}_f^{-1}} \quad | \mathbf{x} \rangle = \sqrt{\mathbf{H}_f^{-1}} r_f(\mathbf{x}) \in \mathbb{S}^n$$

The line vectors $\langle \sigma |$, $\langle \mathbf{x} |$ are traditionally called “bras”, and the column vectors $| \sigma \rangle$, $| \mathbf{x} \rangle$ are called “kets”. The same objects will be denoted in a less abstract vector form:

$$\hat{\boldsymbol{\mu}} = \begin{bmatrix} \hat{\mu}_1 \\ \vdots \\ \hat{\mu}_n \end{bmatrix} = \sqrt{\mathbf{H}_f^{-1}} \boldsymbol{\mu} \quad (43)$$

$$\hat{r}(\mathbf{x}) = \begin{bmatrix} \hat{r}_1(\mathbf{x}) \\ \vdots \\ \hat{r}_n(\mathbf{x}) \end{bmatrix} = \sqrt{\mathbf{H}_f^{-1}} r_f(\mathbf{x})$$

The transformation $\boldsymbol{\mu} \rightarrow \hat{\boldsymbol{\mu}}$ or $\mathbf{r}_f \rightarrow \hat{\mathbf{r}}$ amounts to recombining the measurements linearly in order to have the identity matrix as the covariance matrix of the measurement anticipations:

$$\overline{\hat{\boldsymbol{\mu}}^t \hat{\boldsymbol{\mu}}} = \mathbf{I} \quad (44)$$

5 The function $\hat{r}_i(\mathbf{x})$ is the concentration adjoint, for $(\cdot)_f$ or $\langle \cdot \rangle_f$, to the measurement $\hat{\boldsymbol{\mu}}_i$. For the recombined adjoint functions \hat{r}_i the Gram covariance matrix becomes $\hat{\mathbf{H}} = \mathbf{I}$.

The notation (42) amounts to commonly describe positions and sources by measurement coordinates thus suggesting an equivalence. The vector $|\mathbf{x}\rangle$ corresponds, by definition, to any source producing a measurement vector $\hat{\mathbf{r}}(\mathbf{x}) = \sqrt{\mathbf{H}_f^{-1}} \mathbf{r}_f(\mathbf{x})$. It may be described in particular by the release $\delta_{f\mathbf{x}}$ of a unit amount of tracer from the space time position \mathbf{x} : $\delta_{f\mathbf{x}}(\mathbf{y}) = \frac{\delta(\mathbf{y}-\mathbf{x})}{\rho f(\mathbf{x})}$. The usual Dirac function at point \mathbf{x} is divided by the geometric weight. We may write $|\mathbf{x}\rangle = |\delta_{f\mathbf{x}}\rangle$. The vector $|\mathbf{x}\rangle$ may be similarly described by infinitely many other distributions provided the resulting recombined measurements are $\mathbf{r}_f(\mathbf{x})$. Such a vector as $|\mathbf{x}\rangle$ will be termed a positional ket.

15 The source vector $|\sigma\rangle$ can be any element of \mathbb{R}^n . A positional vector $|\mathbf{x}\rangle$ undergoes two constraints. Firstly it must be obtained as $\sqrt{\mathbf{H}_f^{-1}} \mathbf{r}_f(\mathbf{x})$ from a $\mathbf{r}_f(\mathbf{x})$ with non-negative elements. Secondly as we shall see, $|\mathbf{x}\rangle$ is on the unit sphere.

The scalar product $\langle \cdot \rangle_f$ will now be denoted for two sources σ and σ' :

$$\langle \sigma | \sigma' \rangle = \langle \sigma, \sigma' \rangle_f \quad (45)$$

20 With these notations we obtain for source or positional vectors $|\sigma\rangle$, $|\sigma'\rangle$, $|\mathbf{x}\rangle$ and $|\mathbf{y}\rangle$:

$$\langle \sigma | \sigma' \rangle = {}^t \hat{\boldsymbol{\mu}} \hat{\boldsymbol{\mu}}' = {}^t \boldsymbol{\mu} \mathbf{H}_f^{-1} \boldsymbol{\mu}' \quad (46)$$

$$\langle \mathbf{x} | \mathbf{y} \rangle = {}^t \hat{\mathbf{r}}(\mathbf{x}) \hat{\mathbf{r}}(\mathbf{y}) = {}^t \mathbf{r}_f(\mathbf{x}) \mathbf{H}_f^{-1} \mathbf{r}_f(\mathbf{y})$$

These definitions clearly renounce doing anything with the part σ_{\perp} of the source orthogonal to the adjoint concentrations.

Emergence of a linear tracer source from air concentration measurements

J.-P. Issartel

Title Page

Abstract

Introduction

Conclusions

References

Tables

Figures

⏪

⏩

◀

▶

Back

Close

Full Screen / Esc

Print Version

Interactive Discussion

The pivotal point is the form taken by the entropic constraint (29) for a positional vector:

$$\langle \mathbf{x} | \mathbf{x} \rangle = 1 \quad (47)$$

Due to this entropic normalisation the space-time position vectors $|\mathbf{x}\rangle$ are analogous to the pure states of a quantum system. It is now justified to investigate more accurately the connections between data assimilation and the statistical formalism of the quantum theory. The present approach to quantum formalism will follow the first chapter of the presentation by Kholevo (1980). The presentation by Fano (1967) is also simple for a reader not familiar with this theory.

A source $|\sigma\rangle = \hat{\mu}$ may be decomposed as $|\sigma\rangle = \int \sigma_{||f}(\mathbf{y}) |\mathbf{y}\rangle \rho f d\mathbf{y}$. After noticing that $\sigma_{||f}(\mathbf{y}) = \langle \sigma | \mathbf{y} \rangle$, this decomposition may be put in a form equivalent to Eq. (19):

$$|\sigma\rangle = \int |\mathbf{y}\rangle \langle \mathbf{y} | \sigma \rangle \rho f(\mathbf{y}) d\mathbf{y} \quad (48)$$

As already mentioned the positional ket $|\mathbf{x}\rangle$, tied to a unit release in \mathbf{x} can be represented by the Dirac distribution $\delta_{f,\mathbf{x}}(\mathbf{y})$. According to Eq. (48) it is equivalent as well to the smooth distribution $\delta_{f,\mathbf{x}||}(\mathbf{y}) = \langle \mathbf{x} | \mathbf{y} \rangle$. The combination of the Eqs. (47) and (48) leads to:

$$\int \langle \mathbf{x} | \mathbf{y} \rangle^2 \rho f(\mathbf{y}) d\mathbf{y} = 1 \quad (49)$$

In this equation $f(\mathbf{y}) \langle \mathbf{x} | \mathbf{y} \rangle^2$ is the density of informational energy of the source $|\mathbf{x}\rangle = \delta_{f,\mathbf{x}||}$ per unit mass by the position \mathbf{y} . This may be regarded as well as a probability distribution of the unit amount of energy of $|\mathbf{x}\rangle$. In the renormalised geometry of the known domain described in Sect. 10 the factor f will be eliminated but the probability will still be per unit mass because, in this paper, the density ρ has always been separated from the geometric discussion. Due to Eq. (49) the ket $|\mathbf{x}\rangle$, i.e. the function $\delta_{f,\mathbf{x}||}(\mathbf{y}) = \langle \mathbf{x} | \mathbf{y} \rangle$ is analogous to a wave function of the quantum theory.

Emergence of a linear tracer source from air concentration measurements

J.-P. Issartel

Title Page

Abstract

Introduction

Conclusions

References

Tables

Figures

◀

▶

◀

▶

Back

Close

Full Screen / Esc

Print Version

Interactive Discussion

A source σ will be represented by, or seen as, a linear combination $\sigma_{||f} = |\sigma\rangle$ of the functions \hat{r}_i or r_{fi} adjoint to the measurements $\hat{\mu}_i$ or μ_i . Let's denote $|i\rangle$ the kets associated to the \hat{r}_i and $|r_{fi}\rangle$ the kets tied to the r_{fi} . They are described by the following vectors of recombined measurements:

$$|1\rangle = \begin{bmatrix} 1 \\ 0 \\ \vdots \\ 0 \end{bmatrix}, \dots, |n\rangle = \begin{bmatrix} 0 \\ \vdots \\ 0 \\ 1 \end{bmatrix} \quad |r_{fi}\rangle = \sqrt{\mathbf{H}_f} |i\rangle \quad (50)$$

The family $|1\rangle, \dots, |n\rangle$ is an orthonormal basis of \mathbb{R}^n with which the estimate may be simply written as $|\sigma\rangle = \sum \hat{\mu}_i |i\rangle$. The family $|r_{f1}\rangle, \dots, |r_{fn}\rangle$ is a basis too but it is not orthonormal and the expression for $|\sigma\rangle = \sum \lambda_{fi} |r_{fi}\rangle$ is not so straightforward.

8. States and observables

The symbol $|x\rangle\langle x|$ may be extracted from the Eq. (48) as designating an operator transforming $|\sigma\rangle$ into $\sigma_{||f}(x) |x\rangle$. This operator is a projector because it is self adjoint and $|x\rangle\langle x|x\rangle\langle x| = |x\rangle\langle x|$. This introduces the following definition. Any source ket $|\sigma\rangle$ or positional ket $|x\rangle$ is tied to a state:

$$\mathbf{S}_\sigma = |\sigma\rangle\langle\sigma| \quad \mathbf{S}_x = |x\rangle\langle x| \quad (51)$$

These new objects correspond to the “states” of the statistical quantum theory. The kets $|\sigma\rangle$ and $|x\rangle$ may be thought of vectors so that the states \mathbf{S}_σ and \mathbf{S}_x may be thought of as positive symmetric matrices. As already mentioned \mathbf{S}_x is a one dimensional projector and so is $\langle\sigma|\sigma\rangle^{-1} \mathbf{S}_\sigma$. In particular the entropic constraint (47) or (29) becomes:

$$\text{tr } \mathbf{S}_x = 1 \quad (52)$$

This is indeed the definition of a pure state; $\langle\sigma|\sigma\rangle^{-1} \mathbf{S}_\sigma$ is also a pure state as $\text{tr } \mathbf{S}_\sigma = \langle\sigma|\sigma\rangle$. The states belong to the set $\mathcal{S}_n(\mathbb{R})$ of the self adjoint operators described

by symmetric matrices. This set must be endowed, to describe its role, with the trace scalar product:

$$\begin{aligned} \mathcal{S}_n(\mathbb{R}) : \mathbf{X} \in \mathbb{R}^n \times \mathbb{R}^n, \quad \mathbf{X} = {}^t \mathbf{X} \\ \langle \mathbf{X}, \mathbf{Y} \rangle = \text{tr} \mathbf{XY} \end{aligned} \quad (53)$$

It is easy to show the equivalence of the following systems of equations; for instance

$$\begin{aligned} \langle \mathbf{S}_i, \mathbf{S}_\sigma \rangle = \text{tr} \{ |\sigma\rangle \langle \sigma| i \rangle \langle i| \} = \langle \sigma| i \rangle^2 \\ \mathbf{S}_i = |i\rangle \langle i| \quad 2\mathbf{T}_{i,j} = |i\rangle \langle j| + |j\rangle \langle i| \\ \left\{ \begin{aligned} \langle \sigma| i \rangle = \hat{\mu}_i \\ i = 1, \dots, n \end{aligned} \right\} \iff \left\{ \begin{aligned} \langle \mathbf{S}_i, \mathbf{S}_\sigma \rangle = \hat{\mu}_i^2 \\ \langle \mathbf{T}_{i,j}, \mathbf{S}_\sigma \rangle = \hat{\mu}_i \hat{\mu}_j \\ i = 1, \dots, n \quad j = 1, \dots, n \end{aligned} \right. \end{aligned} \quad (54)$$

This can be formulated in terms of the measurements μ_i :

$$\begin{aligned} \mathbf{S}_{r_{fi}} = |r_{fi}\rangle \langle r_{fi}| \quad 2\mathbf{T}_{r_{fi}, r_{fj}} = |r_{fi}\rangle \langle r_{fj}| + |r_{fj}\rangle \langle r_{fi}| \\ \left\{ \begin{aligned} \langle \sigma| r_{fi} \rangle = \mu_i \\ i = 1, \dots, n \end{aligned} \right\} \iff \left\{ \begin{aligned} \langle \mathbf{S}_{r_{fi}}, \mathbf{S}_\sigma \rangle = \mu_i^2 \\ \langle \mathbf{T}_{r_{fi}, r_{fj}}, \mathbf{S}_\sigma \rangle = \mu_i \mu_j \\ i = 1, \dots, n \quad j = 1, \dots, n \end{aligned} \right. \end{aligned} \quad (55)$$

The operators \mathbf{S}_i , $\mathbf{T}_{i,j}$ and $\mathbf{S}_{r_{fi}}$, $\mathbf{T}_{r_{fi}, r_{fj}}$ correspond to the observables of the quantum theory, respectively associated to the evaluation of the physical quantities $\hat{\mu}_i^2$, $\hat{\mu}_i \hat{\mu}_j$ and μ_i^2 , $\mu_i \mu_j$. The observables are the operators self adjoint for the product $\langle \cdot, \cdot \rangle_f$; they are tied to the symmetric matrices of $\mathcal{S}_n(\mathbb{R})$.

The positional states $\mathbf{S}_x = |x\rangle \langle x|$, for $x \in \Omega \times T$, make up a special class $\mathcal{S}_{\Omega \times T}$ of observables. They are associated to the evaluation of the quantities $\langle \mathbf{S}_x, \mathbf{S}_\sigma \rangle = \sigma_{|f}^2(x)^2$ not to be mistaken for $\sigma(x)^2$ if the real source σ is known to be different from $\sigma_{|f}$.

Emergence of a linear tracer source from air concentration measurements

J.-P. Issartel

Title Page

Abstract

Introduction

Conclusions

References

Tables

Figures

◀

▶

◀

▶

Back

Close

Full Screen / Esc

Print Version

Interactive Discussion

Emergence of a linear tracer source from air concentration measurements

J.-P. Issartel

Title Page

Abstract

Introduction

Conclusions

References

Tables

Figures

⏪

⏩

◀

▶

Back

Close

Full Screen / Esc

Print Version

Interactive Discussion

The equivalent systems on the left and right parts of the expressions (54) or (55) are surprisingly parallel. We propose the following interpretation that should be strengthened by further investigations. In $\Omega \times T$, $r_{fi}(\mathbf{x}) = \langle r_{fi} | \mathbf{x} \rangle$ is the concentration adjoint for $\langle \cdot, \cdot \rangle_f$ indicating the response of the measurement μ_j to a unit amount of tracer released from \mathbf{x} . The same thing may be said in $\mathcal{S}_n(\mathbb{R})$. Indeed the equation $\int \langle \mathbf{S}_x, \mathbf{S}_y \rangle \rho f(\mathbf{y}) d\mathbf{y} = 1$ may be interpreted as the release of a unit amount of informational energy from the position \mathbf{S}_x . The positional states are the Dirac functions of $\mathcal{S}_{\Omega \times T}$ with the trace product. The response of the measurements μ_j^2 , $\mu_j \mu_j$ is then described by $\langle \mathbf{S}_{f_{fi}}, \mathbf{S}_x \rangle$ and $\langle \mathbf{T}_{f_{fi}, f_{fj}}, \mathbf{S}_x \rangle$ that might be written in the functional form of $\mathbf{S}_{f_{fi}}(\mathbf{S}_x)$, $\mathbf{T}_{f_{fi}, f_{fj}}(\mathbf{S}_x)$. So, in $\mathcal{S}_n(\mathbb{R})$ the operators $\mathbf{S}_{f_{fi}}$ and $\mathbf{T}_{f_{fi}, f_{fj}}$ behave like concentrations of informational energy adjoint to the quadratic measurements μ_j^2 , $\mu_j \mu_j$ for the trace product $\langle \cdot, \cdot \rangle$. Correspondingly \mathbf{S}_σ corresponds to the source of a quadratic tracer, the informational energy $\langle \mathbf{S}_\sigma, \mathbf{S}_x \rangle = \mathbf{S}_\sigma(\mathbf{S}_x) = \langle \sigma | \mathbf{x} \rangle^2$. Of course, this interpretation should be complemented by an investigation of the transport equation of this new tracer in $\mathcal{S}_{\Omega \times T}$. This will be left for the future. This interpretation could also be considered to explain a very surprising computational fact. The position and date of the ETEX release are restored in terms of informational energy with a much better accuracy than in terms of the tracer of interest, the perfluoromethylcyclohexane. This is clear on Figs. 5b, d, f, h, 6b, d and, to a lesser extent 6f, h. These figures are drawn in the ordinary geometry where the density of informational energy is described by $f(\mathbf{x})\sigma(\mathbf{x})^2$. The result is even clearer in the renormalised geometry of Figs. 7 and 8 where the density is simply $\sigma(\mathbf{x})^2$.

The use of the statistical formalism of the quantum theory in the description of a macroscopic system as such, regardless of its microscopic structure, is rather surprising. It must be noted that in the present development this use is independent of any hypothesis that the tracer or its energy might decompose into elementary packets. Without judging in advance for further investigations, this remark must be an element of the comparison between data assimilation and quantum theory as the hypothesis of quantization is central in the quantum statistics.

Emergence of a linear tracer source from air concentration measurements

J.-P. Issartel

Title Page

Abstract

Introduction

Conclusions

References

Tables

Figures

◀

▶

◀

▶

Back

Close

Full Screen / Esc

Print Version

Interactive Discussion

© EGU 2004

The present development does not give a meaning to complex valued measurements μ_j . If this was to be done the scalar products $(\cdot, \cdot)_f$, $\langle \cdot, \cdot \rangle_f$ of $\Omega \times T$ and $\langle \cdot, \cdot \rangle$ of $\mathcal{S}_n(\mathbb{R})$ should be replaced by hermitian products. In the formula (55), then, μ_i^2 and $\mu_i \mu_j$ would be replaced respectively by $\mu_i \mu_i^*$ and $(\mu_i \mu_j^* + \mu_i^* \mu_j)/2 = \Re(\mu_i \mu_j^*)$; the stars indicate complex conjugates.

9. Statistical mixtures

The definitions and concepts presented in Sects. 8 and 7 may be handled to describe the effect of measurement uncertainties on the estimate $\sigma_{\parallel f} = |\sigma\rangle = \sum \hat{\mu}_i |i\rangle$. Suppose that, due to some experimental uncertainties, the values of the measurements must be represented with some noise as $\mu_i + \delta\mu_i$ or $\hat{\mu}_i + \delta\hat{\mu}_i$. There must be some probability distribution law $p(\delta\hat{\mu})$ obeyed by the error in such a way that $\int p(\delta\hat{\mu}) d\delta\hat{\mu} = 1$.

We may suppose the error vanishes in the average: $\overline{\delta\hat{\mu}} = \int \delta\hat{\mu} p(\delta\hat{\mu}) d\delta\hat{\mu} = 0$. In this expression the bar is a reference to the statistical law of $\delta\hat{\mu}$, no longer to the law of the expectable values of $\hat{\mu}$. The source estimate becomes uncertain as well, an uncertainty that is readily described. Let's denote the source tied to the average value $\hat{\mu}$ as $\sigma_{\parallel f} = \hat{\mu}$. The source estimated from $\hat{\mu} + \delta\hat{\mu}$ is $\sigma_{\delta\hat{\mu}} = |\sigma_{\delta\hat{\mu}}\rangle = \sigma_{\parallel f} + \delta\hat{\mu}$, its value in x is $\langle \sigma_{\delta\hat{\mu}} | x \rangle = \sigma_{\parallel f}(x) + \delta\sigma_{\parallel f}(x)$ with $\delta\sigma_{\parallel f}(x) = \langle \delta\hat{\mu} | x \rangle$. The variance of the estimate variation for two space time points x and y is obtained by averaging the product:

$$\begin{aligned} \delta\sigma_{\parallel f}(x) \delta\sigma_{\parallel f}(y) &= \langle \delta\hat{\mu} | x \rangle \langle \delta\hat{\mu} | y \rangle \\ &= \text{tr} \{ |x\rangle \langle y| \delta\hat{\mu} \} \langle \delta\hat{\mu} \rangle \end{aligned} \quad (56)$$

This leads to introduce the covariance operator for the measurement errors:

$$\hat{Q} = \int |\delta\hat{\mu}\rangle \langle \delta\hat{\mu}| p(\delta\hat{\mu}) d\delta\hat{\mu} \quad (57)$$

This operator may be simply regarded as the positive symmetric covariance matrix previously introduced in Sect. 4 in terms of the errors $\delta\mu$. According to Eq. (43),

Emergence of a linear tracer source from air concentration measurements

J.-P. Issartel

Title Page

Abstract

Introduction

Conclusions

References

Tables

Figures

◀

▶

◀

▶

Back

Close

Full Screen / Esc

Print Version

Interactive Discussion

$\delta\hat{\boldsymbol{\mu}} = \sqrt{\mathbf{H}_f^{-1}} \delta\boldsymbol{\mu}$, the following identity may be written:

$$\mathbf{Q} = \overline{\delta\boldsymbol{\mu}^t \delta\boldsymbol{\mu}} \quad \hat{\mathbf{Q}} = \overline{\delta\hat{\boldsymbol{\mu}}^t \delta\hat{\boldsymbol{\mu}}} = \sqrt{\mathbf{H}_f^{-1}} \mathbf{Q} \sqrt{\mathbf{H}_f^{-1}} \quad (58)$$

Then the variance of the estimate errors may be written as:

$$\begin{aligned} \overline{\delta\sigma_{\parallel f}(\mathbf{x})^2} &= \langle \mathbf{S}_x, \hat{\mathbf{Q}} \rangle \\ &= {}^t \hat{\mathbf{r}}(\mathbf{x}) \hat{\mathbf{Q}} \hat{\mathbf{r}}(\mathbf{x}) \\ &= {}^t \mathbf{r}_f(\mathbf{x}) \mathbf{H}_f^{-1} \mathbf{Q} \mathbf{H}_f^{-1} \mathbf{r}_f(\mathbf{x}) \end{aligned} \quad (59)$$

The covariance may be evaluated as:

$$\begin{aligned} \overline{\delta\sigma_{\parallel f}(\mathbf{x}) \delta\sigma_{\parallel f}(\mathbf{y})} &= {}^t \hat{\mathbf{r}}(\mathbf{x}) \hat{\mathbf{Q}} \hat{\mathbf{r}}(\mathbf{y}) \\ &= {}^t \mathbf{r}_f(\mathbf{x}) \mathbf{H}_f^{-1} \mathbf{Q} \mathbf{H}_f^{-1} \mathbf{r}_f(\mathbf{y}) \end{aligned} \quad (60)$$

It is more convenient to perform the practical calculation of the errors by means of the expressions implying \mathbf{r}_f and \mathbf{Q} . The experimental errors are generally uncorrelated, $\overline{\delta\mu_i \delta\mu_j} = 0$ for $i \neq j$, so that \mathbf{Q} is a diagonal matrix unlike $\hat{\mathbf{Q}}$. If the model errors were included in $\delta\boldsymbol{\mu}$, of course \mathbf{Q} would no longer be diagonal. This situation is not considered in the present paper. For the ETEX experiments the relative uncertainty of the measurements was evaluated to 15% (Joint Res. Centre, 1998). The variance $\overline{\delta\sigma_{\parallel f}(\mathbf{x})^2}$ represented on Figs. 7b and 8b were calculated for a relative Gaussian uncertainty of 30%. This means a diagonal covariance matrix was handled:

$$\mathbf{Q} = 0.09 \begin{bmatrix} \mu_1^2 & & \\ & \ddots & \\ & & \mu_n^2 \end{bmatrix} \quad (61)$$

It must be stressed that the variance (59) and covariance (60) are by no means an evaluation of $\sigma_{\perp f}$. As already said in the Sect. 6 from the point of view of the monitoring

Emergence of a linear tracer source from air concentration measurements

J.-P. Issartel

Title Page

Abstract

Introduction

Conclusions

References

Tables

Figures

⏪

⏩

◀

▶

Back

Close

Full Screen / Esc

Print Version

Interactive Discussion

network $\sigma_{\perp f}$ is exactly as if it did not exist and this point of view would be ours if we could put all our information in the evaluation of $\sigma_{\parallel f}$. The above variance and covariance just describe the uncertainty of the estimate stemming from the uncertainty of the measurements. It is accordingly natural to see that the variance evaluated on Figs. 7b3bis and 8b3bis are not representative for the huge local difference between the ETEX1 point release and its estimate.

The uncertainty of the estimate is usually described by the background covariance matrix \mathbf{B} and by the kernel (24). This kernel does not coincide with the expressions (59) and (60). The reason is that a clear distinction has been stated in Sect. 3 between the covariance matrix of the measurement errors $\overline{\delta\boldsymbol{\mu}^t \delta\boldsymbol{\mu}} = \mathbf{Q}$ and the covariance matrix of the measurement anticipations $\overline{\boldsymbol{\mu}^t \boldsymbol{\mu}}$, the latter being hypothetically identified in Sect. 4 as $\overline{\boldsymbol{\mu}^t \boldsymbol{\mu}} = \mathbf{H}_f$. In other words the following distinction is established by the present development between the estimation errors and the expectable sources:

$$\overline{\delta\sigma_{\parallel f}(\mathbf{x})\delta\sigma_{\parallel f}(\mathbf{y})} \neq \overline{\sigma_{\parallel f}(\mathbf{x})\sigma_{\parallel f}(\mathbf{y})} \quad (62)$$

In this expression the left and right bars have totally different meanings. The left bar refers to the statistics of the measurement errors tied to the technological quality of the detectors. The right bar refers to the measurement anticipations assumed to be statistically tied to the geometric arrangement of the detectors.

In quantum statistics the situation defined by uncertain measurements is associated to a mixed state \mathbf{S} :

$$\mathbf{S} = \int |\sigma_{\delta\hat{\boldsymbol{\mu}}}\rangle \langle\sigma_{\delta\hat{\boldsymbol{\mu}}}| \rho(\delta\hat{\boldsymbol{\mu}}) d\delta\hat{\boldsymbol{\mu}} = \mathbf{S}_{\sigma_{\parallel f}} + \hat{\mathbf{Q}} \quad (63)$$

The mixed state or mixture \mathbf{S} is still a positive symmetric operator but it is no longer proportional to a one dimensional projector or pure state as are the $\mathbf{S}_{\sigma_{\delta\hat{\boldsymbol{\mu}}}} = |\sigma_{\delta\hat{\boldsymbol{\mu}}}\rangle \langle\sigma_{\delta\hat{\boldsymbol{\mu}}}|$. This is an important tool of the statistical theory. In the present case the variance may be represented as:

$$\overline{\delta\sigma_{\parallel f}(\mathbf{x})^2} = \langle \mathbf{S}, \mathbf{S}_x \rangle - \langle \mathbf{S}_{\sigma_{\parallel f}}, \mathbf{S}_x \rangle$$

$$= \overline{\sigma_{\delta\hat{\mu}}(\mathbf{x})^2} - \overline{\sigma_{\delta\hat{\mu}}(\mathbf{x})}^2 \quad (\overline{\sigma_{\delta\hat{\mu}}} = \sigma_{\parallel f}) \quad (64)$$

10. Geometric considerations

The transformation $\mathbf{x} \mapsto |\mathbf{x}\rangle = \hat{\mathbf{r}}(\mathbf{x})$ may be regarded as a mapping or coordinate change sending $\Omega \times T$ onto a four-dimensional submanifold of \mathbb{S}^n . This submanifold, endowed with its ordinary Euclidean geometry, gives the best natural account of the information. We shall show that, indeed, no renormalisation is necessary for this geometry.

To this end let's denote this submanifold as \mathcal{C} and as $d\hat{\mathbf{r}}$ the Euclidean four dimensional element of \mathcal{C} around a point $\hat{\mathbf{r}} = \hat{\mathbf{r}}(\mathbf{x})$. The notation $d|\mathbf{x}\rangle$ would be acceptable but disconcerting. The link between $d\mathbf{x}$ and $d\hat{\mathbf{r}}$ implies the Jacobian function g of the transformation: $d\mathbf{x} = g(\hat{\mathbf{r}})d\hat{\mathbf{r}}$. We then obtain the expression (65) for the recombined i th measurement. The notation $(\cdot)_{fg}^{\mathcal{C}}$ just states that due to the change of coordinate and integration domain, the form of the measurement product is changed. In $\Omega \times T$ a renormalising function f was used with respect to the Euclidean element $d\mathbf{x}$, in \mathcal{C} the renormalising function is fg with respect to the Euclidean element $d\hat{\mathbf{r}}$.

$$\begin{aligned} \hat{\mu}_i &= \int_{\Omega \times T} \sigma \hat{r}_i f \rho d\mathbf{x} = (\sigma, \hat{r}_i)_f \\ &= \int_{\mathcal{C}} \sigma \hat{r}_i f g \rho d\hat{\mathbf{r}} = (\sigma, \hat{r}_i)_{fg}^{\mathcal{C}} \end{aligned} \quad (65)$$

The functional dependence of $\rho(\mathbf{x})$, $f(\mathbf{x})$, $\sigma(\mathbf{x})$ and $\hat{r}_i(\mathbf{x})$ is just transferred from \mathbf{x} to $\hat{\mathbf{r}}$: $\rho(\hat{\mathbf{r}})$, $f(\hat{\mathbf{r}})$, $\sigma(\hat{\mathbf{r}})$ and $\hat{r}_i(\hat{\mathbf{r}})$. In the case of \hat{r}_i the transfer is excessively simple $\hat{r}_i(\hat{\mathbf{r}}) = \hat{r}_i$. This just means that the function adjoint to the i th measurement for the product $(\cdot)_{fg}^{\mathcal{C}}$ is the i th coordinate of $\hat{\mathbf{r}}$. Of course the abstract notation $\hat{r}_i(\hat{\mathbf{r}})$ will no longer be used, \hat{r}_i is enough.

The change of coordinate for the source domain does not change the form of the Gram matrix. Indeed, the scalar product $(\hat{r}_i, \hat{r}_j)_{fg}^{\mathcal{C}}$ of \hat{r}_i, \hat{r}_j as functions of $\hat{\mathbf{r}}$ is the same

Emergence of a linear tracer source from air concentration measurements

J.-P. Issartel

Title Page

Abstract

Introduction

Conclusions

References

Tables

Figures

⏪

⏩

◀

▶

Back

Close

Full Screen / Esc

Print Version

Interactive Discussion

Emergence of a linear tracer source from air concentration measurements

J.-P. Issartel

Title Page

Abstract

Introduction

Conclusions

References

Tables

Figures

⏪

⏩

◀

▶

Back

Close

Full Screen / Esc

Print Version

Interactive Discussion

as $(\hat{r}_i, \hat{r}_j)_f$ where \hat{r}_i, \hat{r}_j are considered functions of x . This matrix is the identity as stated by the expression (44): $\hat{H}_f = \hat{H}_{fg}^C = \overline{\hat{\mu}^t \hat{\mu}} = \mathbf{I}$.

As the probability distribution of the expectable measurement values is still optimal, the illumination still undergoes the constraint (29) which means that ${}^t \hat{r} \hat{H}_{fg}^C \hat{r} f(\hat{r}) g(\hat{r}) = 1$.

5 As $\hat{H}_{fg}^C = \mathbf{I}$ we already know that ${}^t \hat{r} \hat{r} = \langle x | x \rangle = 1$. This implies, as announced $f g \equiv 1$.

The geometry of \mathcal{C} cannot be represented on a sheet of paper. The main problem is that \mathcal{C} is embedded in \mathbb{R}^n . This geometry was obtained from the ordinary geometry by attributing the point x of the ordinary domain $\Omega \times T$ a weight $f(x)$. It is possible to obtain a satisfactory account of this selected property. We just have to find some mapping from \mathbb{R}^4 into itself with f as Jacobian function. The Figs. 3, 4, 7 and 8 were built as follows. As the source was investigated at the surface Σ of the ground or oceans, the working domain was in fact $\Sigma \times T$. Then, for some selected moment t_0 we obtained an illumination $f(x, y, t_0)$. For the Figs. 3 and 4 the illumination was averaged on 24-h periods. It was then very easy to obtain a two-dimensional transformation of Σ with the given Jacobian $f(x, y, t_0)$. To this end the Cartesian coordinates (x, y) are first replaced by polar coordinates (l, θ) for some given centre. Then, with θ kept unchanged, l is transformed into l' according to the following differential equation which provides the adequate transformation of the surface and time element:

$$dl'^2 = f(l, \theta, t_0) dl^2 \quad (66)$$

$$d\theta l' dl' dt = f(l, \theta, t_0) d\theta dl dt$$

20 The representation obtained this way is just an approximation of the known domain but it emphasises several points.

Firstly, the known domain is finite. Its total weight is the number of measurements. On the distorted maps obtained for Europe on Figs. 3, 4, 7, 8 an edge or horizon is clearly visible.

25 Secondly the illumination is important but finite and non singular in the space-time neighbourhood of the detectors. This produces flare shaped excrescences on the fig-

Emergence of a linear tracer source from air concentration measurements

J.-P. Issartel

[Title Page](#)[Abstract](#)[Introduction](#)[Conclusions](#)[References](#)[Tables](#)[Figures](#)[⏪](#)[⏩](#)[◀](#)[▶](#)[Back](#)[Close](#)[Full Screen / Esc](#)[Print Version](#)[Interactive Discussion](#)

ures. No flare is visible on the Figs. 3a1bis, a2bis, b1bis, b2bis corresponding to periods of time with no active detector. In the very geometry of C each flare corresponds to a deep cone with, locally, a symmetric arrangement around a detector in the bottom of the cone.

5 Thirdly there is an intermediate region between the “deep” detectors and the remote horizon. In this region the distortion is not so big and the European coastline is well identifiable.

Fourthly the regions away from the detectors become smaller and smaller. We think this corresponds to the well known conic illusion that a remote object looks smaller. The coast of Iceland, of the Iberian peninsula, of Scandinavia finally become a chaotic zigzag along the horizon. This is illustrated by the Fig. 4. A source of tracer there will be more and more difficult to capture with the measurements.

10 The approximate representation for the known domain puts all the distortion on the space coordinates (x, y) . It should be noted that in the finite geometry of C the distortion with respect to the ordinary geometry necessarily touches t as well. The following arguments even suggest a severe contraction of the time close to the horizon. The measurements performed for ETEX cover a period of time of 90 h. The adjoint functions r_{fi} of these measurements behave like retroplumes transported back in time by the winds and scattered by the diffusion. Due to the diffusion, the regions far away will have been passed over by the retroplumes during periods of time all the larger than the original 90 h as they lie further away from the monitoring network. This means in turn that the 90-h measurements will have captured a part of existence of these remote regions representing more, possibly much more, than 90 hours. Just as if, by sitting in the countryside for one hour and looking far enough, we could see a tree growing from a seed, have fruits and die. One may for instance consider that, at times preceding the states represented on Fig. 3a1 and b1, the illumination extends through the Atlantic ocean to North America. At these times the retroplumes are so flattened and homogenised that their ability to discriminate the structural details of a source there and then is purely residual. Accordingly the contribution to the known domain by the

long passing of the adjoint functions above this continent should reduce to a tiny spot. Due to the scarcity of the information in the space-time regions close to the horizon, the very structure of a source there is lost in practice. The image of the growing tree was idealised: with the logical connections mostly cancelled by the scarcity of the information, we would rather see a chaotic agitation of seeds, fruits and branches.

11. Calculations about ETEX1

The experiment ETEX, sponsored by the European Commission, was organised in 1994. A extensive description is given in (Joint Res. Centre, 1998). It was originally aimed, after the Chernobyl event in 1986, at validating the dispersion models that would be involved in forecasting the extension of a polluted plume. A first release ETEX1 was performed near the village of Monterfil, 2° 00' W, 48° 03' N, Brittany, France. At ground level 340 kg of an inert tracer, perfluoromethylcyclohexane or pmch, were emitted on October 1994, between 23, 16:00 UT and 24, 4:00 UT. All over Europe 168 detectors delivered three hourly averaged concentration measurements. These data are available from the Joint Research Centre, Environment Monitoring Unit, Ispra (Varese), Italy (web site <http://java.ei.jrc.it/etex/database/>). The second release ETEX2 performed later in November was considered less successful.

The calculations proposed here, related to ETEX1, were achieved for two selections of 51 measurements performed by 6 detectors and 137 measurements performed on a wider area and longer duration by 14 detectors. The measurements of the first selection are included in the second one except for half of those performed close to Monterfil by the station F2. These selections with the concentrations really observed are presented on the Fig. 1. The stations and measurements were chosen in order to capture the evolution of the plume of pmch with its edges. In particular, the series of zero measurements taken by the station F8, Brest, should indicate a western limit of the reconstructed release. This limit is not obtained so clearly in the calculations because the series of measurements began at 13:00 UT, just three hours before the release.

Emergence of a linear tracer source from air concentration measurements

J.-P. Issartel

Title Page

Abstract

Introduction

Conclusions

References

Tables

Figures

⏪

⏩

◀

▶

Back

Close

Full Screen / Esc

Print Version

Interactive Discussion

Emergence of a linear tracer source from air concentration measurements

J.-P. Issartel

[Title Page](#)[Abstract](#)[Introduction](#)[Conclusions](#)[References](#)[Tables](#)[Figures](#)[⏪](#)[⏩](#)[◀](#)[▶](#)[Back](#)[Close](#)[Full Screen / Esc](#)[Print Version](#)[Interactive Discussion](#)

Data collected earlier would have indicated zero concentrations so that it would be justified to use artificial measurements. We did not do it and the lack of data before 23 October 1994, 13:00 UT is expected to harm the quality of the inversion for the early period.

5 In a first stage the adjoint concentrations r_i were calculated in pure advection-diffusion with the model POLAIR and stored hourly at ground level. The calculation was performed on a grid extending from 25° W to 30° E and from 43° N to 68° N with a resolution of 0.5°×0.5°. Fifteen Cartesian levels were used with boundaries at 0, 50, 100, 200,..., 2300, 2600, 3000 m above ground or sea level. The calculations with time reversal extended from 27 October 1994, 7:00 UT back to 19 October 1994, 0:00 UT
10 with a 15-min step. The six-hourly meteorological data were produced by and obtained from the European Centre for Mediumrange Weather Forecast with the kind agreement of Météo France. The diffusion was parametrised according to [Louis \(1979\)](#) and [Louis et al. \(1982\)](#). POLAIR ([Sartelet et al., 2002](#); [Sportisse et al., 2002](#); [Boutahar et al., 2003](#)) is the fruit of a close cooperation with the team in charge at Electricité de
15 France of the passive atmospheric transport model Diffeul ([Wendum, 1998](#)). It is a fully modular 3-D Eulerian chemistry transport model. Advection is solved with a flux limiter method; diffusion is solved by a three point scheme. An general account of the numerical treatment of the diffusion was given by [Ouahsine and Smaoui \(1999\)](#). Each adjoint
20 concentration required 2 mn CPU time on a PC (Pentium IV, 2.8 GHz, 1 Go RAM).

In a second stage the inversion was performed according to the method developed in this paper for a surface source at ground or sea level. It was applied on a smaller area extending between 24.5° W to 23.5° E and from 43.5° N to 67.5° N with a resolution of 0.5°×0.5° and one hour. Five sets of data were used:

- 25 1. synthetic values μ^s calculated by POLAIR for both selections of measurements and for the source ETEX1
2. real values μ from the ETEX1 database for both selections
3. synthetic values μ^g calculated by POLAIR for the selection of 137 measurements

and for an imaginary widespread Gaussian source

The reconstruction of a Gaussian source was prepared in order to investigate the potential of the method with respect to the widespread sources for which it is primarily designed. The Gaussian source was placed in a space time region of good illumination with a centre at 8° E, 49° N in space, on 24 October 1994, 10:00 UT in time, six hours after the end of the ETEX release. The total amount of the release was again 340 kg for characteristic length and duration $l_0=165$ km, $\tau=18$ h. This imaginary release was accordingly proportional to the Gaussian distribution $\gamma(l, t)$ for a distance l and a date t measured from the centre:

$$\gamma(l, t) = \frac{e^{-\frac{1}{2} \left\{ \frac{l^2}{l_0^2} + \frac{t^2}{\tau^2} \right\}}}{(2\pi)^{\frac{3}{2}} \tau^{\frac{1}{2}} l_0} \quad (67)$$

The preliminary step of the inversion was the iterative calculation of the optimal renormalising function. A covariance matrix \mathbf{H}_{f_0} was first calculated with a renormalising function $f_0(\mathbf{x}) \equiv 1$ equivalent to no renormalisation at all. A renormalising function was obtained, $f_1(\mathbf{x}) \equiv f_0(\mathbf{x}) \sqrt{r_{f_0} \mathbf{H}_{f_0}^{-1} r_{f_0}}$, in order to prepare a renormalised covariance matrix \mathbf{H}_{f_1} . After nine iterations of type (35) the optimal renormalising function was obtained with $0.985 \leq r_{f_9} \mathbf{H}_{f_9}^{-1} r_{f_9} \leq 0.995$. The inversion of the symmetric matrices was regularised by a Truncated Singular Value Decomposition (Bertero et al., 1985, 1988; Fan et al., 1999). The inversion of the little eigenvalues was topped in order to maintain a conditioning less than 900.

Then the source estimate $\sigma_{||f}$ was obtained by calculating $\mathbf{H}_{f_9}^{-1} \boldsymbol{\mu}$. The variance of this estimate $\overline{\delta \sigma_{||f}(\mathbf{x})^2} = r_{f_9} \mathbf{H}_{f_9}^{-1} \mathbf{Q} \mathbf{H}_{f_9}^{-1} r_{f_9}$ was calculated, as described in Sect. 9, for a relative Gaussian uncertainty of 30% corresponding to the covariance matrix (61).

Finally an estimate σ_f^+ was calculated according to the method described in (Issartel, 2003). The reader is reminded that this estimate is everywhere non negative, satisfies the measurements and, under these constraints, its norm, i.e. here $(\sigma_f^+, \sigma_f^+)_f$ is minimal.

Emergence of a linear tracer source from air concentration measurements

J.-P. Issartel

Title Page

Abstract

Introduction

Conclusions

References

Tables

Figures

◀

▶

◀

▶

Back

Close

Full Screen / Esc

Print Version

Interactive Discussion

Note that in this case: $(\sigma_f^+, \sigma_f^+)_f > \langle \sigma_f^+, \sigma_f^+ \rangle_f$. The calculation is based on the conjecture that:

$$\sigma_{||f}(x) \leq 0 \xrightarrow{?} \sigma_f^+(x) = 0, \quad x \in \Omega \times T \quad (68)$$

Despite the result always successfully passes the necessary and sufficient optimality conditions of Karush, Kuhn and Tucker (Rockafellar, 1970), the conjecture was proved false by J.-B. Baillon (University Paris 1) with a counter example reported in (Issartel, 2003).

The images in the renormalised geometry were prepared in vector format. The vectorial images are defined with an accuracy independent of the visualisation tools by contours, and the contours are defined as polygons by a list of points. In our case the contours were tied to the coast lines and to function levels. The energy and estimate variance levels had to be extracted from the ordinary geometry, a point for which we received the help of Geoffray Adde and Fabien Lejeune as indicated in the comments of Fig. 8. Each point of the contours was then moved according to the Eq. (66). To this end the function f calculated with a space grid 96×48 was interpolated on a much thinner grid 672×336 .

The calculation time for the inversion with 51 measurements was 2 mn 30 s CPU on a PC (Pentium IV, 2.8 GHz, 1 Go RAM). With 137 measurements this time becomes 20 min. Most of this time is devoted to the iterative calculation of the renormalising function. The calculation of the algebraic and positive estimates was organised in order to require then a few additional seconds.

In addition, for comparison purpose, a series of more traditional inversions was performed with Gaussian base functions γ_j of the form (67). Each γ_j was centred by the space time position of the measurement μ_j with characteristic length and duration $l_0 = 165$ km, $\tau = 18$ h. The source was obtained in the form of $\sigma_{est}(x) = \sum \lambda_j \gamma_j(x, t)$ after inverting a measurement matrix $\lambda = H^{-1} \mu$. In that case, nevertheless, the matrix H of elements $h_{i,j} = \int \rho r_i \gamma_j d\mathbf{x}$ is not symmetric. For a point source the method is divergent. In order to investigate the behaviour of this strategy, in particular its divergence for

Emergence of a linear tracer source from air concentration measurements

J.-P. Issartel

Title Page

Abstract

Introduction

Conclusions

References

Tables

Figures

⏪

⏩

◀

▶

Back

Close

Full Screen / Esc

Print Version

Interactive Discussion

little scale sources, it was applied to synthetic values of the selection of 137 measurements and for seven imaginary Gaussian sources. These sources were all centred by the space time position of the ETEX release with characteristic lengths and durations, smaller, equal or larger than those of the γ_i as indicated on the Fig. 10.

12. Results

The results obtained from the calculations described in the previous section for the estimation of the source ETEX1 may be summarised as follows. The Fig. 2 is a comparison of the results obtained with the ordinary geometry and with a geometry transformed by the optimal renormalising function. The illumination, algebraic and positive estimates are integrated in time for both selections of synthetic measurements, without or with renormalisation. The comparison of the Figs. 2a1 and b1 or c1 and d1 shows a much better and wider distribution of the illumination in the renormalised case. Contrary to our expectation, the optimised illumination is not flat around the monitoring network. It still displays peaks, though no longer singular, around the detectors. The quality of the renormalised estimates is clearly improved. The maximum releases are no longer obtained by the positions of the detectors, they are found close to Monterfil. The magnitude of the total amount is now correct, closer to 340 kg in the positive case.

The Fig. 3 illustrates the geometric meaning of the illumination which coincides, in the optimal case, with the renormalising function. The time evolution of the known domain \mathcal{C} is represented for five successive days by the flat approximations corresponding to radial transformation centred at Monterfil, except for the Fig. 3b5ter. The known domain is finite, limited by a space time horizon in red on the figures. The effect of aperture from the Figs. 3a1bis to a3bis or b1bis to b3bis illustrates as well its finite extent in the past. The known domain is finite towards the future, nothing is known after the end of the last measurement. This shutting is visible on the Fig. 3a5bis. The comparison of the parts a and b illustrates the influence of a greater number of measurements. In particular the second selection still includes a lot of measurement for the fifth period and the

Emergence of a linear tracer source from air concentration measurements

J.-P. Issartel

Title Page

Abstract

Introduction

Conclusions

References

Tables

Figures

⏪

⏩

◀

▶

Back

Close

Full Screen / Esc

Print Version

Interactive Discussion

**Emergence of a linear
tracer source from air
concentration
measurements**

J.-P. Issartel

[Title Page](#)[Abstract](#)[Introduction](#)[Conclusions](#)[References](#)[Tables](#)[Figures](#)[⏪](#)[⏩](#)[◀](#)[▶](#)[Back](#)[Close](#)[Full Screen / Esc](#)[Print Version](#)[Interactive Discussion](#)

known domain is still widely open. At that moment the illuminated cloud is shifted to the north east and a radial transformation centred in the Danish islands produces on the Fig. 3b5ter lesser distortions than may be seen in b5bis.

The finite extension of the known domain does not mean that finitely many regions are seen by the measurements. It means that large, possibly infinitely large remote regions of the space time domain will be attributed a residual information weight. As an illustration Iceland is reduced on the Fig. 4 to a thin zigzag along the horizon, close to Ireland.

The five day periods were chosen to almost completely include that space time extent of the sources rebuilt from the ETEX data. The reader may consider the Figs. 5 and 6 with the idea that there is no significant release of tracer at times preceding the period d_0-2 days or following the period d_0+2 days. As already shown by the Fig. 3 the region of Monterfil is much better seen during the period after the release than before the release. The quality of the algebraic sources rebuilt on the Figs. 5 and 6 is much better for the periods including and following the real twelve hour release. The tracer contribution from the early poorly seen regions is overestimated. This aberrations may be compared to the impossibility to estimate the distances and the real dimensions of the stars with the naked eyes. In other words the overestimation of the first two periods would mean that there is not enough information in the selections of measurements to decide between a smaller close source or a bigger one further away. A valuable correction is brought by the positivity constraint. More surprisingly the representation of the informational energy displays a very peaked structure by the space time position of the very release. This may be understood because in the ordinary geometry the density of energy $f\sigma^2$ is a compromise including the renormalising or illumination function weak during the first two periods. The comparison of the Figs. 5 and 6 mainly shows that, due to a greater number of measurements the reconstruction from the real data is subject to more model errors. These are seen on the subfigures f4, f5, h4, h5 in the form of peaks of energy by the positions of the detectors.

For the synthetic inversions the focus of the energy in the appropriate part of the

Emergence of a linear tracer source from air concentration measurements

J.-P. Issartel

[Title Page](#)[Abstract](#)[Introduction](#)[Conclusions](#)[References](#)[Tables](#)[Figures](#)[⏪](#)[⏩](#)[◀](#)[▶](#)[Back](#)[Close](#)[Full Screen / Esc](#)[Print Version](#)[Interactive Discussion](#)

known domain is even clearer in the renormalised geometry of the Figs. 7, 8, part a. Note that the total duration covered by these figures is 48 h instead of 120 for the previous ones. The comparison of the Figs. 7a3, a4, and 8a3, a4 indicate a better focus in time for the selection of 51 measurements and in space for the selection of 137 measurements. The most interesting comparison is between the part b of the figures describing the variance of the estimate as a result of measurement errors representing 30% of the signal. This variance is, roughly, one order of magnitude below the informational energy. It is visibly less, by roughly a factor three, in the case of the greatest number of measurements. Hence it may be concluded that the difference on the Figs. 5 and 6 between the sources rebuilt out of synthetic measurements and out of real measurements is due mostly to the model errors.

The algebraic and positive reconstructions of a widespread source on the Fig. 9 does not significantly drift from the above conclusions. Note that the colour scale chosen for this figure is flatter than that used for the Figs. 6 and 7 so that the defaults are emphasised. The general features of the source are recovered, the total amount of the release for each period is retrieved within a factor two. There is still an overestimation of the early releases, when the illumination is low. Again this aberration is mostly corrected by the positivity constraint. It must be noted that the quality of the estimate is better in the close environment of the active detectors. This is very visible with the deep low valued indentation tied to the station F8, Brest, on the subfigures b3, b4, c3, c4.

The Fig. 10 shows time integrated sources rebuilt from synthetic measurements with Gaussian base functions with characteristic length and duration $l_0=165$ km, $\tau=18$ h. The sources are also Gaussian, centred with a total release of 340 kg by the space time position of the ETEX release. The characteristic lengths and durations of these sources were varied, nevertheless, from $l_0=69$ km, $\tau=7$ h 30 min to $l_0=440$ km, $\tau=48$ h. When the characteristic elements of the source coincide with those of the base functions, the inversion, as shown by the subfigure d, is satisfactory. The source is retrieved with a spatial resolution consistent with the Gaussian length. As might be expected

Emergence of a linear tracer source from air concentration measurementsJ.-P. Issartel

[Title Page](#)[Abstract](#)[Introduction](#)[Conclusions](#)[References](#)[Tables](#)[Figures](#)[⏪](#)[⏩](#)[◀](#)[▶](#)[Back](#)[Close](#)[Full Screen / Esc](#)[Print Version](#)[Interactive Discussion](#)

© EGU 2004

the subfigure a shows that a combination of finitely many Gaussian functions cannot produce a Dirac. The divergence of the method at the lowest scales is not surprising. The apparent divergence at the high scales is more surprising on the subfigure g. The complete time evolution of the estimate g , not shown, displays important negative releases at and around the position of Monterfil during the period corresponding to the release. So, it seems that Gaussian base functions might not be adequate for the observation of the large scale structures. We think, but this should be further supported, that an effect of the renormalisation is to optimise the base functions with respect to all space and time scales. In particular, as emphasised by the calculations about ETEX1, the inversion strategy proposed in this paper is not divergent for this point source.

13. Discussion and perspectives

The inverse technique proposed in this paper processes at once all the measurements available at all times in order to retrieve a source σ_{if} with its complete time evolution. In this respect, it could be classified four-dimensional variational assimilation (Bouttier and Courtier, 1999). The evaluation of the estimation errors follows nevertheless an unusual scheme resulting from the distinction proposed between the measurement anticipations and the measurement errors. This evaluation is illustrated by the Figs. 7 and 8. The simultaneous assimilation of all the data will lead to a problem when their number will be daily increased by the operation of a regular network. The difficulty may probably be solved reasonably, and the results presented here show it is worth trying.

The definition of a “known domain” is both natural and useful. It is natural because the intuition perfectly agrees that the relevance of a set of data cannot extend indefinitely. And it is a useful diagnostics about the sufficiency and adequacy of a monitoring network. The known domain is a strange object. The measurements are combined to produce an estimate regardless of the precedence of the ones compared to the others. The idea of a time flying seems to vanish. In the known domain what would be the

Emergence of a linear tracer source from air concentration measurements

J.-P. Issartel

[Title Page](#)[Abstract](#)[Introduction](#)[Conclusions](#)[References](#)[Tables](#)[Figures](#)[⏪](#)[⏩](#)[◀](#)[▶](#)[Back](#)[Close](#)[Full Screen / Esc](#)[Print Version](#)[Interactive Discussion](#)

meaning of a ket $|x\rangle$ “before” a ket $|y\rangle$? Keys would probably arise from an investigation of the form taken by the transport equation of the tracer after the transformation from the ordinary geometry. A transport equation should also be established, as suggested in Sect. 8 for the informational energy. These investigations will require a better representation of the known domain than the above flat radial transformations. It seems that the complete description of its four-dimensional geometry embedded in a higher dimension is a matter of tensor analysis (Raschewski, 1953).

The effect of the model errors has been evaluated in the calculations but it was not considered in the theory. As this error was shown preponderant compared to the experimental one the gap must be filled in the future. The usual solution amounts to considering the model errors as a particular kind of measurement errors. In that case the corresponding covariance matrix will have to be evaluated; unlike the experimental errors these errors will be correlated for the various measurements and the matrix will not be diagonal.

The search of the source under positive condition, a hypothesis relevant for ETEX, was shown to significantly improve the quality of the estimate. The sources investigated in meteorology often display slow variations in space and time. Sometimes they display predictable daily or seasonal variations. This additional information must be taken into account and it is taken into account by the implementations of data assimilation based on Kalman’s filtering (Rödenbeck et al., 2003; Anderson and Moore, 1979). This may certainly be done in the framework of the present paper. The work will amount to determining in this respect the logical status of the additional information.

It must be noted that the increasing development of non linear chemistry transport models (Mallet and Sportisse, 2004) is a field of application of inverse techniques, in the hypothesis of linear perturbations. In the case of the present strategy, this would mean that the link is linear between the expectable mismatch of the sought source compared to an a priori estimate on the one hand and on the other hand the expectable mismatch of the measurements compared to their a priori values.

The word “renormalisation” was chosen by analogy with the theory of quantum elec-

rodynamics where it designates the removal of an unphysical infinity by means of an infinite additive correction.

Acknowledgements. The author is deeply grateful to B. Sportisse for his trust, to L. Gallardo-Klenner, A. Baklanov, M. Bocquet, A. Ouahsine and G. Roussel for their encouragement, to S. Lacour, G. Adde, F. Lejeune, J. Louchet, V. Mallet and W. M. Okia for their advice. Graphics have been prepared with the user friendly and public domain graphical package named GrADS originally developed by B. Dotty (COLA, support@grads.iges.org) and maintained with the help of M. Fiorino (LLNL).

References

- Anderson, B. D. O. and Moore, J. B.: Optimal filtering, Prentice-Hall Information and System Sciences Series, edited by Kailath, T., Prentice-Hall, Inc., 1979. [2655](#)
- Ashbaugh, L. L., Malm, W. C., and Sadeh, W. Z.: A residence time probability analysis of sulfur concentrations at Grand Canyon National park, Atmos. Environ., 19, (8), 1263–1270, 1985. [2617](#)
- Baklanov, A.: Modelling of the atmospheric radionuclide transport: local to regional scale, Numerical Mathematics and Mathematical Modelling, INM RAS, Moscow, volume 2, (special issue dedicated to 75-year jubilee of academician G. I. Marchuk), 244–266, 2000. [2617](#)
- Baklanov, A. and Mahura, A.: Assessment of possible airborne impact from risk sites: methodology for probabilistic atmospheric studies, Atmos. Chem. Phys., 3, 485–495, 2004. [2616](#)
- Bertero, M., de Mol, C., Pike, and E. R.: Linear inverse problems with discrete data, I: General formulation and singular system analysis, II: Stability and regularisation, Inverse Problems, 1, 301–330, 1985 (part I) and 4, 573–594, 1988 (part II). [2649](#)
- Bousquet, P., Peylin, P., Ciais, P., Rayner, P., Friedlingstein, P., Lequere, C., and Tans, P.: Inter-annual CO₂ sources and sinks as deduced by inversion of atmospheric CO₂ data, Science, 290, 1342–1346, 2000. [2616](#)
- Boutahar, J., Lacour, S., Mallet, V., Quélo, D., Roustan, Y., and Sportisse, B.: Development and validation of a fully modular platform for the numerical modeling of air pollution: POLAIR, accepted for publication in International Journal of Environment and Pollution, 2004. [2648](#)
- Bouttier, F. and Courtier, P.: Data assimilation concepts and methods, March 1999, available on the web site: http://www.ecmwf.int/newsevents/training/rcourse_notes/

Emergence of a linear tracer source from air concentration measurements

J.-P. Issartel

Title Page

Abstract

Introduction

Conclusions

References

Tables

Figures

⏪

⏩

◀

▶

Back

Close

Full Screen / Esc

Print Version

Interactive Discussion

DATA_ASSIMILATION/ASSIM_CONCEPTS/Assim_concepts21.html, Meteorological training course lecture series, printed 2001. [2617](#), [2654](#)

Brandt, J., Ebel, A., Elbern, H., Jakobs, H., Memmesheimer, M., Mikkelsen, T., Thykier-Nielsen, S., and Zlatev, Z.: The importance of accurate meteorological input fields and accurate planetary boundary layer parameterizations, tested against ETEX-1, in ETEX symposium on long-range atmospheric transport, model verification and emergency response, 13–16 May 1997, Vienna, Austria, edited by Nodop, K., Proceedings, European Commission, EUR 17346 EN, 195–198, 1997. [2618](#)

Cheney, E. W.: Introduction to approximation theory, International series in pure and applied mathematics, McGraw-Hill, 1966. [2617](#)

Clerbaux, C., Hadji-Lazaro, J., Turquety, S., Mégie, G., and Coheur, P.: Trace gas measurements from infrared satellite for chemistry and climate applications, Atmos. Chem. Phys., 3, 1495–1508, 25, 2003. [2616](#)

Enting, I. G., Trudinger, C. M., and Francey, R. J.: A synthesis inversion of the concentration and $\delta^{13}\text{C}$ of atmospheric CO_2 , Tellus, 47B, 35–52, 1995. [2617](#)

Enting, I. G.: Green's function methods of tracer inversion, edited by Kasibhatla, P., Heimann, M., Rayner, P., Mahowald, N., Prinn, R. G., and Hartley, D. E., Inverse methods in global biogeochemical cycles, Geophysical Monograph Series, American Geophysical Union, Washington, D.C., 2000. [2617](#)

Fan, S. M., Sarmiento, J. L., Gloor, M., and Pacala, S. W.: On the use of regularization techniques in the inverse modeling of atmospheric carbon dioxide, J. Geophys. Res., 104, 17, 21 503–21 512, 1999. [2649](#)

Fano, G.: Metodi matematici della meccanica quantistica, Zanichelli, 1967, translated in English as: Mathematical methods of quantum mechanics, edited by Landovitz, L. F., McGraw Hill, 1971. [2637](#)

Gallardo, L., Olivares, G., Langner, J., and Aarhus, B.: Coastal lows and sulfur air pollution in central Chile, Atmos. Environ., 36, 3829–3841, 2002. [2616](#)

Golub, G. H. and Van Loan, C. F.: Matrix computations, The Johns Hopkins University Press, Baltimore, 1983.

Gram, J. P.: Om Rackkændvilklinger bestemte ved Hjaelp af de minfste Kvadraters Methode, Copenhagen, 1879, translated in German as: Über die Entwicklung reeller Funktionen in Reihen mittels der Methode der kleinsten Quadrate, Journal für reihe und angewandte Mathematik, 94, 41–73, 1883. [2617](#)

Emergence of a linear tracer source from air concentration measurements

J.-P. Issartel

Title Page

Abstract

Introduction

Conclusions

References

Tables

Figures

◀

▶

◀

▶

Back

Close

Full Screen / Esc

Print Version

Interactive Discussion

- Hartley, R. V. L.: Transmission of information, Bell System Technical Journal, 7, (3), 535–563, 1928. [2632](#)
- Hatori, H.: A note on the entropy of a continuous distribution, Kodai Mathematical Seminar Reports, 10, 172–176, 1958. [2632](#)
- Hourdin, F. and Issartel, J.-P.: Subsurface nuclear tests monitoring through the CTBT xenon network, Geophys. Res. Lett., 27, (15), 2245–2248, 2000. [2619](#)
- Issartel, J.-P. and Baverel, J.: Inverse transport for the verification of the CTBT, Atmos. Chem. Phys., 3, 475–486, 2003. [2616](#), [2619](#)
- Issartel, J.-P.: Rebuilding sources of linear tracers after atmospheric concentration measurements, Atmos. Chem. Phys., 3, 475–486, 2003. [2617](#), [2620](#), [2649](#), [2650](#)
- Joint Research Centre: Etex, The European tracer experiment, European communities, EUR 18143 EN, ISBN 92-828-5007-2, 107, 1998. [2642](#), [2647](#)
- Kholevo, A. S.: Veroyatnostnye i statisticheskie aspekty kvantovoi teorii, Moskva, Nauka, 1980, translated in English as: Probabilistic and statistical aspects of quantum theory, North Holland Series in Statistics and Probability, volume 1, edited by Krishnaiah, P. R., Rao, C. R., Rosenblatt, M., and Rozanov, Y. A., North Holland, 1982. [2637](#)
- Lorensen, W. E. and Cline, H. E.: Marching cubes: a high resolution 3D surface construction algorithm, Computer Graphics, 21, 3, 163–169, 1987. [2668](#)
- Louis, J.-F.: A parametric model of vertical eddy fluxes in the atmosphere, Boundary Layer Meteorology, 17, 187–202, 1979. [2648](#)
- Louis, J.-F., Tiedke, M., and Geleyn, J.-F.: A short history of the PBL parameterization at ECMWF, Proceedings ECMWF workshop on planetary boundary layer parameterization, 59–79, 1982. [2648](#)
- Mallet, V. and Sportisse, B.: 3-D chemistry-transport model Polair: numerical issues, validation and automatic-differentiation strategy, Atmos. Chem. Phys. Discuss., 4, 1371–1392, 2004. [2655](#)
- Marchuk, G. I.: Sopryazhennye Uravneniya i Analiz Slozhnykh Sistem, Moskva, Nauka, 1992, translated in English as: Adjoint Equations and Analysis of Complex Systems, Mathematics and its Applications, volume 295, edited by Hazewinkel, M., Kluwer Academic Publisher, 1995. [2616](#)
- Marchuk, G. I.: Perturbation theory and the statement of inverse problems, Lecture Notes in Computer Science, v. 4, 159, 1973. [2617](#)
- Marchuk, G. I.: Equation for value of information from meteorological satellites and formulation

Emergence of a linear tracer source from air concentration measurementsJ.-P. Issartel

Title Page

Abstract

Introduction

Conclusions

References

Tables

Figures

◀

▶

◀

▶

Back

Close

Full Screen / Esc

Print Version

Interactive Discussion

**Emergence of a linear
tracer source from air
concentration
measurements**

J.-P. Issartel

[Title Page](#)[Abstract](#)[Introduction](#)[Conclusions](#)[References](#)[Tables](#)[Figures](#)[⏪](#)[⏩](#)[◀](#)[▶](#)[Back](#)[Close](#)[Full Screen / Esc](#)[Print Version](#)[Interactive Discussion](#)

of inverse problems, Space Research, v. 2, no. 3, 462–477, 1964. [2617](#)

Middleton, D.: An Introduction to Statistical Communication Theory, International Series in Pure and Applied Physics, McGraw Hill, p. 307–310, 1960. [2632](#)

5 Ouahsine, A. and Smaoui, H.: Flux-limiter schemes for oceanic tracers: application to the English Channel tidal model, Comput. Methods Appl. Mech. Engrg., 179, 307–325, 1999. [2648](#)

Penenko, V. and Baklanov, A.: Methods of sensitivity theory and inverse modeling for estimation of source term and nuclear risk/vulnerability areas, Lecture Notes in Computer Science (LNCS), Springer, 2074, 57–66, 2001. [2616](#)

10 Penenko, V., Baklanov, A., and Tsvetova, E.: Methods of sensitivity theory and inverse modeling for estimation of source term, Future Generation Computer Systems, 18, 661–671, 2002. [2616](#)

Pudykiewicz, J.: Application of adjoint tracer transport equations for evaluating source parameters, Atmos. Environ., 32, (17), 3039–3050, 1998. [2616](#)

Raschewski, P. K.: Rimanova geometriya i tenzornii analiz, Gostekhizdat, Moskva, 1953, translated in German as: Riemannsche Geometrie und Tensoranalysis, VEB Deutscher Verlag der Wissenschaften, Berlin, 1959. [2655](#)

Rockafellar, R. T.: Convex analysis, Princeton University Press, 1970. [2650](#)

20 Robertson, L. and Persson, C.: Attempts to Apply Four Dimensional Data Assimilation of Radiological Data Using the Adjoint Technique, Radiation Protection Dosimetry, 50, 333–337, 1993. [2616](#)

Rödenbeck, C., Houweling, S., Gloor, M., and Heimann, M.: CO₂ flux history 1982–2001 inferred from atmospheric data using a global inversion of atmospheric transport, Atmos. Chem. Phys., 3, 1919–1964, 2003. [2616](#), [2655](#)

25 Roussel, G., Ternisien, E., and Benjelloun, M.: Estimation d'un modèle stationnaire de dispersion et localisation de source, Application à la surveillance de la pollution, Revue du Traitement du Signal, 19, (1), 37–48, 2002. [2616](#)

Sartelet, K. N., Boutahar, J., Quélo, D., Coll, I., and Sportisse, B.: Development and validation of a 3D chemistry transport model POLAIR3D, by comparison with data from ESQUIF campaign, Proc. of the 6th GLOREAM workshop: Global and Regional Atmospheric Modelling, Aveiro, Portugal, September 4–6, 2002. [2648](#)

30 Seibert, P.: Inverse modelling with a Lagrangian particle dispersion model: application to point releases over limited time intervals, edited by Gryning, S. E. and Schiermeier, F. A., Air

**Emergence of a linear
tracer source from air
concentration
measurements**

J.-P. Issartel

[Title Page](#)[Abstract](#)[Introduction](#)[Conclusions](#)[References](#)[Tables](#)[Figures](#)[⏪](#)[⏩](#)[◀](#)[▶](#)[Back](#)[Close](#)[Full Screen / Esc](#)[Print Version](#)[Interactive Discussion](#)

Pollution and its Application XIV, 381–389, NATO, Kluwer Academic/Plenum Publisher, 2001.

[2616](#), [2618](#)

Shannon, C. E.: A mathematical theory of communication, Bell System Technical Journal, 27, (3), 379–423 and 27, (4), 623–656, 1948. [2632](#)

Sharan, M., McNider, R. T., Gopalakrishnan, S. G., and Singh, M. P.: Bhopal gas leak: a numerical simulation of episodic dispersion, Atmos. Environ., 29, 2051–2059, 1995. [2616](#)

Sportisse, B., Boutahar, J., Debry, E., Quélo, D., and Sartelet, K.: Some tracks in air pollution modeling and simulation, Revista de la Real Academia de Ciencias, Serie A: Matemáticas (RACSAM), 96, (3), 507–528, 2002. [2648](#)

Stohl, A.: Computation, accuracy and applications of trajectories – a review and bibliography, Atmos. Environ., 32, (6), 947–966, 1998. [2617](#)

Tarantola, A.: Inverse problem theory, Elsevier, 1987. [2617](#)

Uliasz, M. and Pielke, R.: Application of the receptor oriented approach in mesoscale dispersion modeling, edited by van Dop, H. and Steyn, D. G., Air Pollution and its Application VIII, 399–407, NATO, Plenum Publisher, 1991. [2617](#)

Wendum, D.: Three long-range transport models compared to the ETEX experiment: a performance study, Atmos. Environ., 32, (24), 4297–4305, 1998. [2618](#), [2648](#)

Wotawa, G., de Geer, L.-E., Denier, P., Kalinowski, M., Toivonen, H., d'Amours, R., Desiato, F., Issartel, J.-P., Langer, M., Seibert, P., Frank, A., Sloan, C., and Yamazawa, H.: Atmospheric transport modelling in support of CTBT verification – overview and basic concepts, Atmos. Environ., 37, 2525–2537, 2003. [2617](#)

Emergence of a linear tracer source from air concentration measurements

J.-P. Issartel

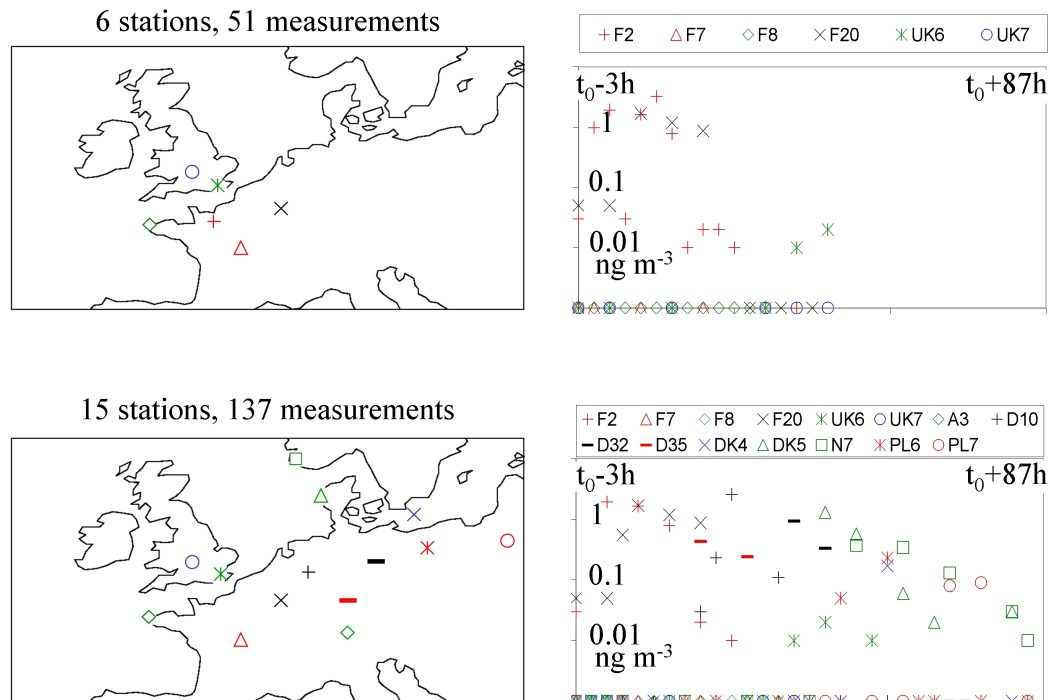


Fig. 1. Geographic and time distribution of the two selections of measurements used for the calculations. Upper two images, the 51 measurement selection, lower two images the 137 measurement selection. The time t_0 corresponds to the beginning of the pmch release in Monterfil, 23 October 1994, 16:00 UT; the first sampling period begins at $t_0-3\text{h}$. Different detectors are indicated by different symbols. The values in ng of pmch per m^3 are from the ETEX1 database.

Title Page

Abstract

Introduction

Conclusions

References

Tables

Figures

◀

▶

◀

▶

Back

Close

Full Screen / Esc

Print Version

Interactive Discussion

Emergence of a linear tracer source from air concentration measurements

J.-P. Issartel

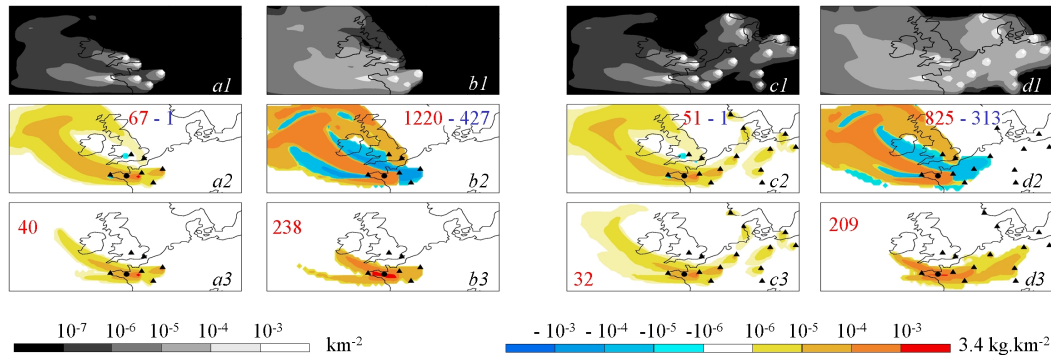


Fig. 2. The figure represents the illumination on the first line, the source rebuilt for the ETEX release as a linear combination of the adjoint functions on the second line, under positivity constraint on the third line; these variables are integrated in time for the whole duration of the calculation. Synthetic values were used for the measurements, 51 in (a) and (b), 137 in (c) and (d). No correction of the illumination is made in (a) nor in (c). The optimal renormalisation was performed for (b) and (d). The red and blue numbers indicate the total amount in kg of the positive and negative releases respectively. The release is indicated by a dot and the detectors by triangles.

Title Page

Abstract

Introduction

Conclusions

References

Tables

Figures

◀

▶

◀

▶

Back

Close

Full Screen / Esc

Print Version

Interactive Discussion

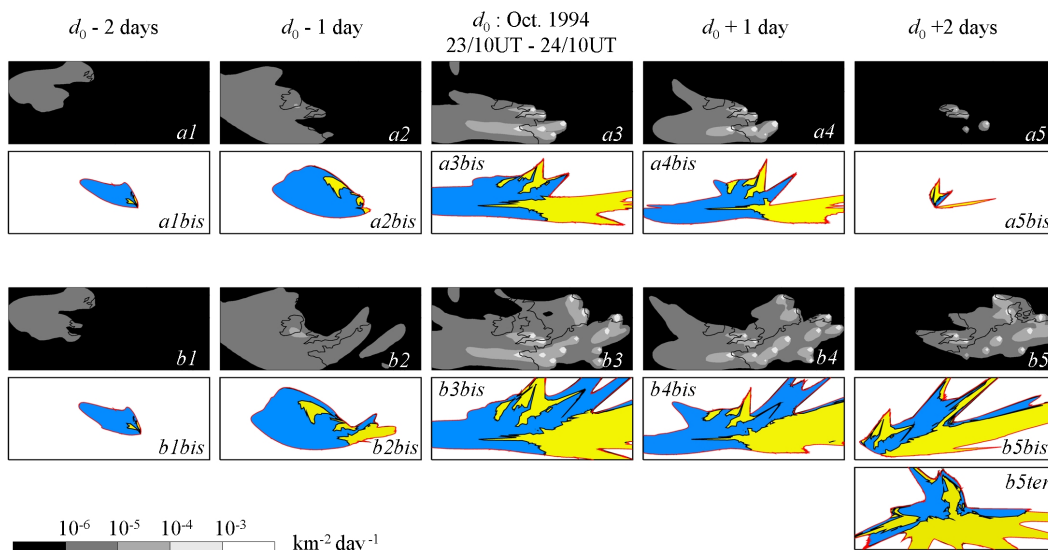


Fig. 3. Evolution of the renormalised illumination for the selections of 51 measurements in **(a)**, 137 in **(b)**. The illumination has been integrated in time for five successive 24-h periods, the third one beginning 6 h before and finishing 6 h after the ETEX release. On the figures **(bis)** this daily integrated illumination is transformed into a geometry by means of a radial transformation centred at Monterfil. The figure **(b5ter)** was obtained with a centre of the radial transformation in the Danish islands. The distortions are less in **(b5ter)** than in **(b5bis)** but the areas of the various regions are the same on both figures.

Emergence of a linear tracer source from air concentration measurements

J.-P. Issartel

Title Page

Abstract

Introduction

Conclusions

References

Tables

Figures

◀

▶

◀

▶

Back

Close

Full Screen / Esc

Print Version

Interactive Discussion

Emergence of a linear tracer source from air concentration measurementsJ.-P. Issartel

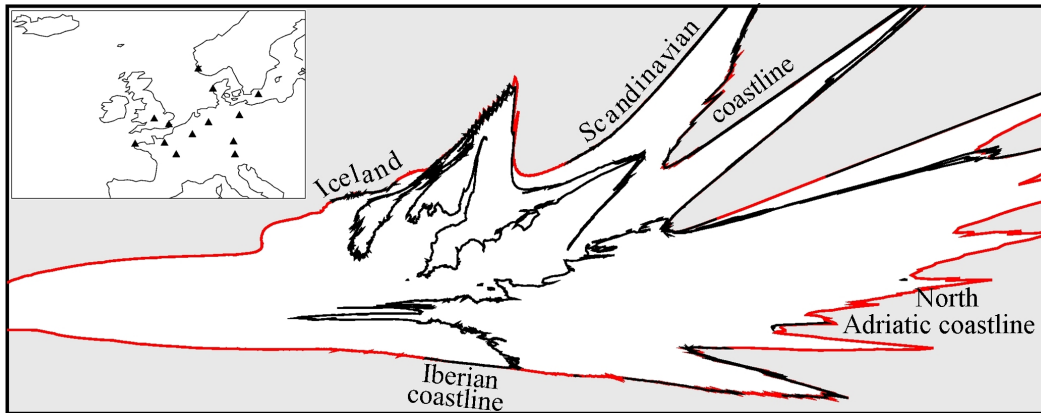


Fig. 4. Enlargement of the Fig. 3 (b3bis) with emphasis to the coastlines in black, especially close to the horizon in red. The regularisation of the coasts has not been activated in order to better show the increasing instability of the calculation close to the horizon. In the subfigure the triangles indicate the detectors operated during the 24-h period (see Fig. 3).

[Title Page](#)[Abstract](#)[Introduction](#)[Conclusions](#)[References](#)[Tables](#)[Figures](#)[⏪](#)[⏩](#)[◀](#)[▶](#)[Back](#)[Close](#)[Full Screen / Esc](#)[Print Version](#)[Interactive Discussion](#)

Emergence of a linear tracer source from air concentration measurements

J.-P. Issartel

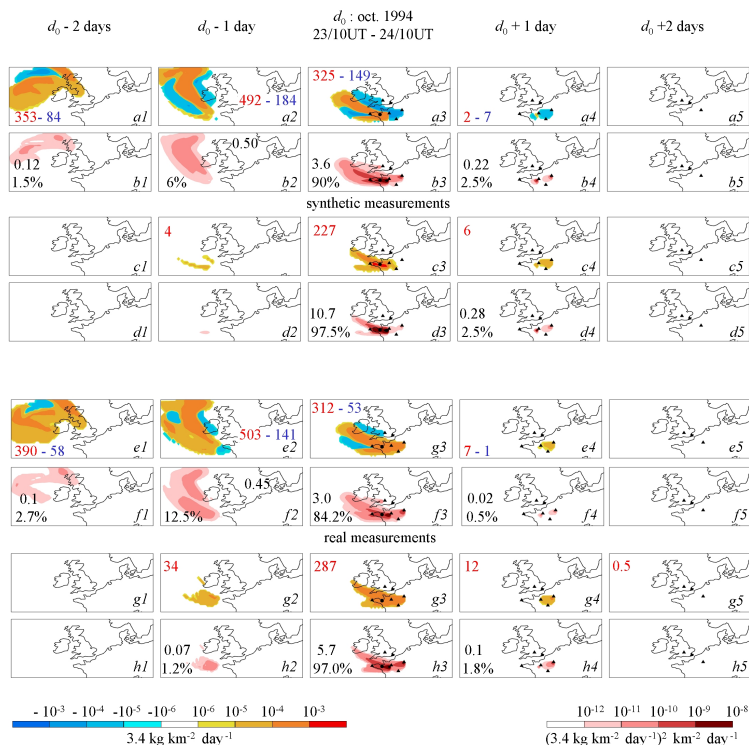


Fig. 5. Daily integrated evolution of the source rebuilt for the ETEX release by means of renormalised adjoint functions. In **(a)** the source rebuilt linearly for synthetic measurements is integrated on 24-h periods, and in **(c)** the source rebuilt under positivity constraints. The red and blue numbers correspond to the total in kg of the positive and negative releases during the successive periods. The energy released by both estimate is integrated on the same periods respectively in **(b)** and **(d)**. This amount is indicated for the five periods as an absolute value in $(3.4 \cdot 10^{-6} \text{ kg km}^{-2} \text{ day}^{-1})$ and as a percentage of the total energy release of the estimate. The dot and the triangles indicate the ETEX release and the detectors when they are active. Figures **(e)**, **(f)**, **(g)**, **(h)** are obtained similarly for the real values from the ETEX1 database.

Title Page

Abstract

Introduction

Conclusions

References

Tables

Figures

◀

▶

◀

▶

Back

Close

Full Screen / Esc

Print Version

Interactive Discussion

Emergence of a linear tracer source from air concentration measurements

J.-P. Issartel

Title Page

Abstract

Introduction

Conclusions

References

Tables

Figures

◀

▶

◀

▶

Back

Close

Full Screen / Esc

Print Version

Interactive Discussion

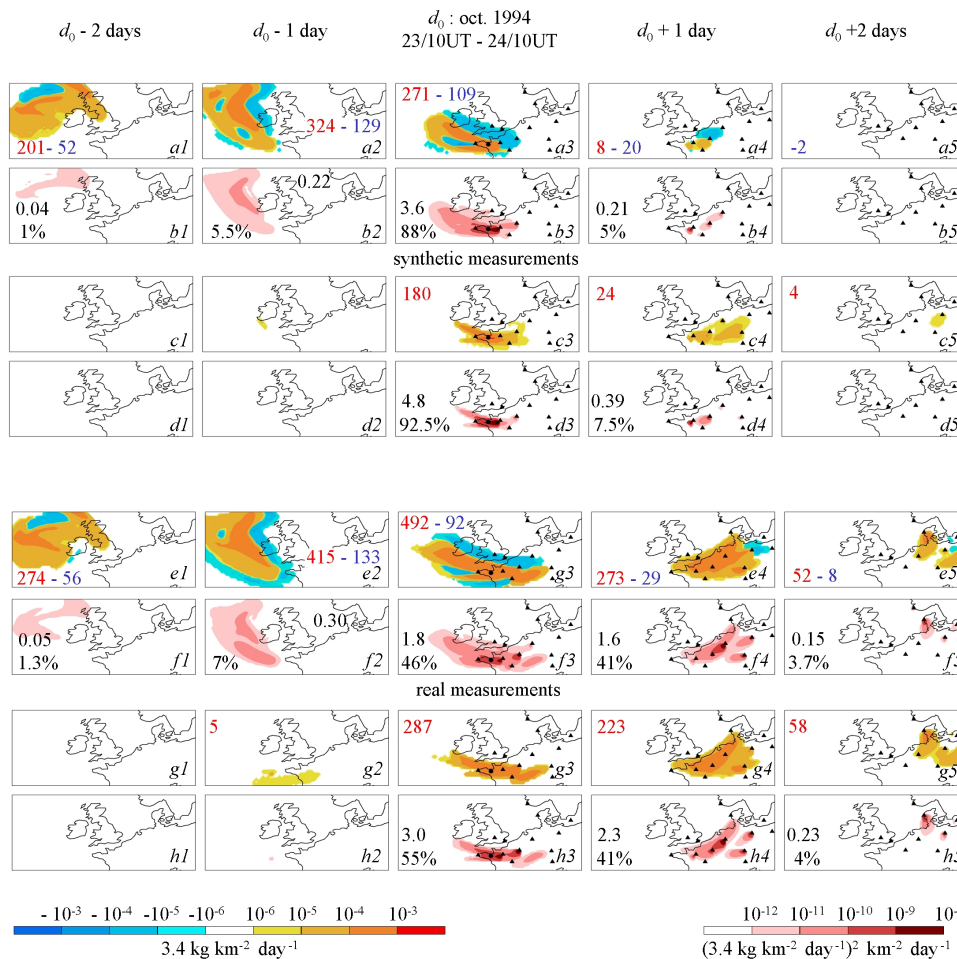


Fig. 6. Results obtained for the selection of 137 measurements. The organisation of this figure is parallel to that of Fig. 5.

Emergence of a linear tracer source from air concentration measurements

J.-P. Issartel

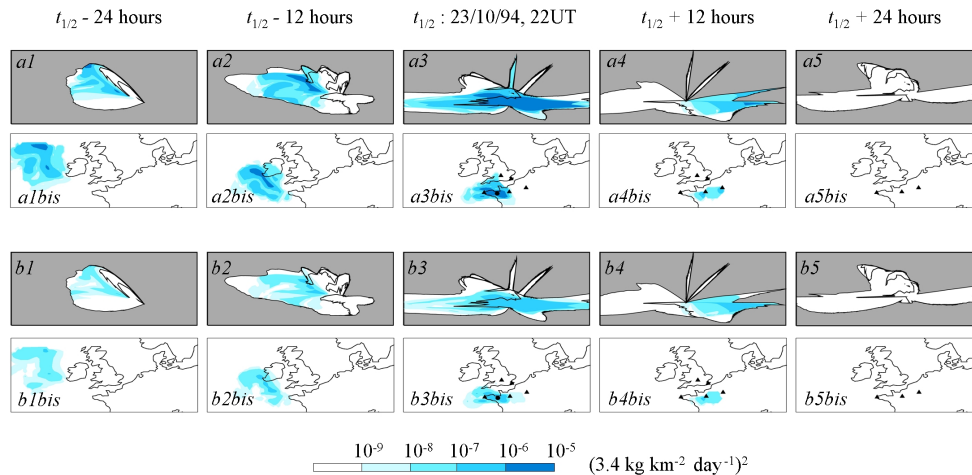


Fig. 7. The space time density of informational energy of a source σ is described by $f\sigma^2$ in the ordinary geometry but in the renormalised geometry of the known domain this density is described by σ^2 . The part **(a)** of the figure describes this density $\sigma_{||}^2$ for the estimate linearly rebuilt out of 51 synthetic ETEX measurements. The part **(b)** shows the variance $\overline{\delta\sigma_{||}^2}$ of this

estimate for 30% of relative Gaussian errors: $\sqrt{\overline{\delta\mu_i^2}} = 0.3\mu_i$. The quantities σ^2 and $\overline{\delta\sigma_{||}^2}$ are represented 12 hourly at five moments without any time integration; the third moment correspond to the middle of the twelve hour ETEX release. The renormalised geometry is accounted for by a radial transformation, centred at Monterfil. As a help, on the figures **(bis)** both quantities are also represented in the ordinary geometry; take care that in this ordinary geometry σ^2 is not a relevant description of the energy. The dot and the triangles indicate the source and the detectors operated at the given moment.

Title Page

Abstract

Introduction

Conclusions

References

Tables

Figures

◀

▶

◀

▶

Back

Close

Full Screen / Esc

Print Version

Interactive Discussion

Emergence of a linear tracer source from air concentration measurements

J.-P. Issartel

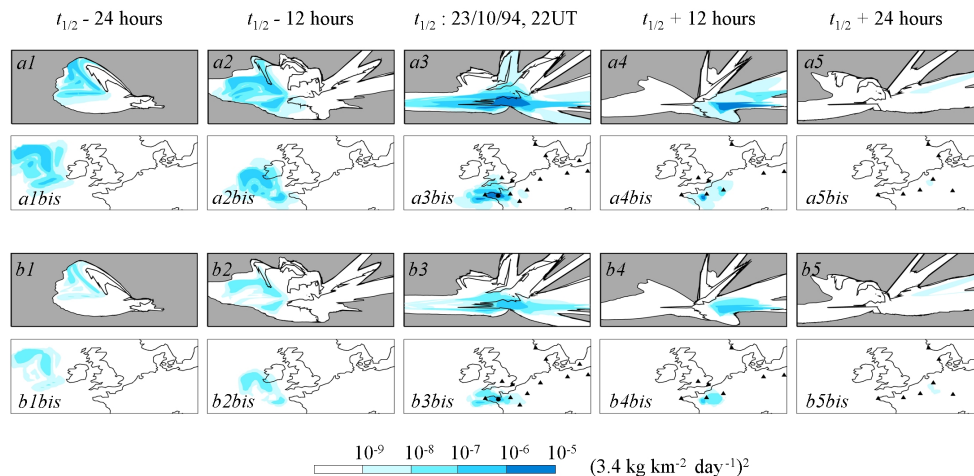


Fig. 8. Results obtained for the selection of 137 measurements. The organisation of this figure is parallel to that of Fig. 7. The extraction of the level contours from the ordinary geometry was kindly programmed, using the marching squares algorithm (Lorenson and Cline, 1987), by Geoffroy Adde and Fabien Lejeune at CERTIS/ENPC.

Title Page

Abstract

Introduction

Conclusions

References

Tables

Figures

◀

▶

◀

▶

Back

Close

Full Screen / Esc

Print Version

Interactive Discussion

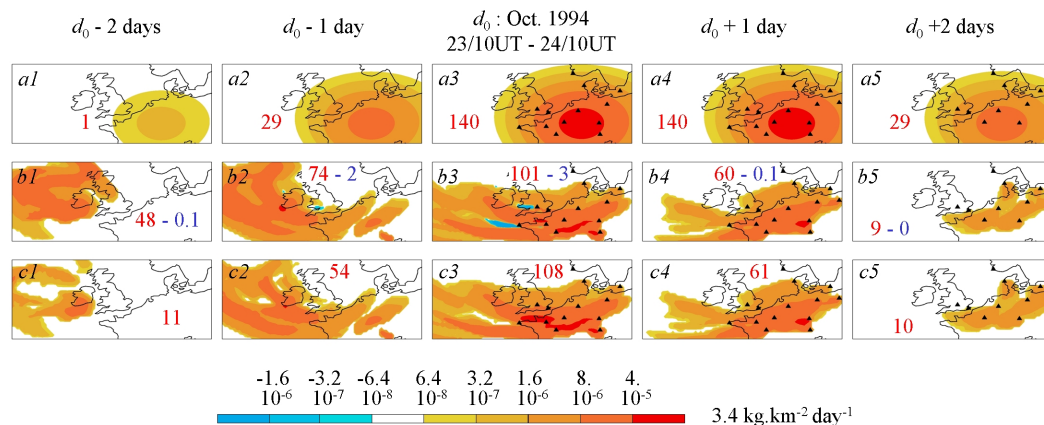


Fig. 9. Reconstruction of a Gaussian surface source with renormalised adjoint functions corresponding to the selection of 137 measurements. The daily integrated evolution of the source to be rebuilt is represented in (a) for five successive 24-h periods. This source is centred in time at 24 October 1994, 10:00 UT. It was centred in space at 8° E, 49° N in order to be symmetrically inserted among the measurement. The characteristic length and duration of this 340 kg Gaussian release were 167 km, 18 h. In (b) and (c) the source is rebuilt respectively without and with a positivity constraints. The red and blue numbers indicating the total amount, in kg, of the positive and negative releases during the successive periods. The triangles indicate the detectors operated during the five periods.

Emergence of a linear tracer source from air concentration measurements

J.-P. Issartel

Title Page

Abstract

Introduction

Conclusions

References

Tables

Figures

◀

▶

◀

▶

Back

Close

Full Screen / Esc

Print Version

Interactive Discussion

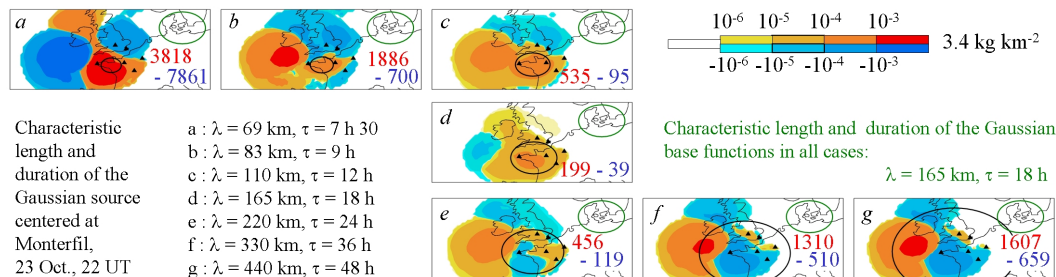


Fig. 10. Synthetic values for the selection of 51 measurements were generated for different characteristic lengths and durations of a Gaussian surface release, with 340 kg of a tracer, centred at Monterfil, 23 October 1994, 22:00 UT. The horizontal extent of the sources to be rebuilt is indicated by a black ellipse. The source was rebuilt as a combination of Gaussian base functions centred by the space time position of each measurement, and with in all cases the same characteristic length, symbolised by the green ellipse, and duration corresponding to the case (d) of the source. The triangles indicate the detectors operated during the five periods. The reconstruction is integrated in time on the figures with red and blue numbers indicating the total amount, in kg, of the positive and negative releases in the solution. The result is satisfactory when the source and the base functions have the same element, otherwise aberrations appear rapidly.

Emergence of a linear tracer source from air concentration measurements

J.-P. Issartel

Title Page

Abstract

Introduction

Conclusions

References

Tables

Figures

◀

▶

◀

▶

Back

Close

Full Screen / Esc

Print Version

Interactive Discussion